Structure-Guided Design, synthesis, and evaluation of 1-Indanone and 1,3-Indandione Derivatives as ligands for Misfolded α-Synuclein Aggregates

Xianwei Sun[†], Prasad Admane[†], Zbigniew A. Starosolski[†,‡], Jason L. Eriksen[§], Ananth V. Annapragada[†,‡], Eric A. Tanifum[†,‡]*.

[†]Department of Radiology, Baylor College of Medicine, Houston, Texas 77030

[‡]Edward B. Singleton Department of Radiology, Texas Children's Hospital, Houston, Texas 77030

[§] College of Pharmacy, Pharmacological and Pharmaceutical Sciences, University of Houston, Houston, Texas 77204

ABSTRACT

The development of imaging agents for in vivo detection of alpha-synuclein (α-syn) pathologies faces several challenges. A major gap in the field is the lack of diverse molecular scaffolds with high affinity and selectivity to α-seen fibrils for in vitro screening assays. Better in vitro scaffolds can instruct the discovery of better in vivo agents. We report the rational design, synthesis, and in vitro evaluation of a series of novel 1-indanone and 1,3-indandione derivatives from a Structure-Activity Relationship (SAR) study centered on some existing

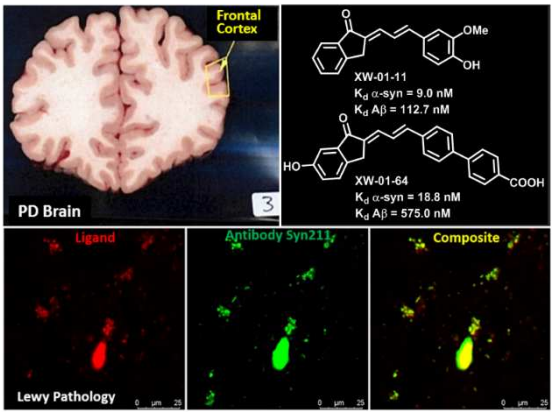

α-seen fibril binding ligands. Our results from fibril saturation binding experiments show that two of the lead candidates bind α-seen fibrils with binding constants (K_d) of 9.0 and 18.8 nM, respectively, and selectivity of greater than 10x for α-seen fibrils compared with amyloid-β (Aβ) fibrils. Our results demonstrate that the lead ligands avidly label all forms of α-seen on PD brain tissue sections, but only the dense core of senile plaques in AD brain tissue, respectively. These results are corroborated by ligand-antibody colocalization data from Syn211, which shows immunoreactivity towards all forms of α-seen aggregates, and Syn303, which displays preferential reactivity towards mature Lewy pathology. Our results reveal that 1-indanone derivatives have desirable properties for the biological evaluation of α-synucleinopathies.

1. Introduction

Pathological deposits of misfolded protein aggregates are a prominent characteristic of neurodegenerative disorders such as Parkinson's disease (PD), Alzheimer's disease (AD), and related dementias [1,2]. PD is the second most common neurodegenerative disease after AD and is characterized clinically by motor symptoms, including bradykinesia, rigidity, tremor, and postural instability[3]. The development of motor symptoms has been shown to correlate with degeneration of dopaminergic neurons in the substantia nigra, accompanied by cytoplasmic deposition of Lewy pathology in the form of Lewy bodies (LB) and Lewy neurites (LN). Lewy pathology is composed primarily of misfolded alpha-synuclein (α-seen) aggregates. The regional distribution of α-seen in PD postmortem

studies suggests that this pathology originates from the olfactory bulb and the lower brain stem and undergoes progressive spread to other areas of the CNS[4,5]. Empirical data also shows abundant LBs and LNs in the medulla oblongata, pontine tegmentum, and anterior olfactory bulb before the manifestation of PD-related motor symptoms[6-8]. Motor symptoms appear at the intermediate stages of the disease, where the pathology has spread to the substantia nigra and other foci within the basal portions of the mid- and forebrain[6].

The correlation of Lewy pathology with nigrostriatal degeneration and motor dysfunction[4,9] in post mortem studies of PD patients suggests that technologies enabling noninvasive detection and quantification of α-seen aggregates could be valuable for early diagnosis and clinical evaluation of Lewy body disorders. Early detection can provide better opportunities for the recruitment of patient cohorts for clinical trials, evaluation of disease-modifying therapies, and validation of new drug candidates' therapeutic efficacy. Some data indicate that as the disease progresses, some PD patients develop dementia, which correlates with other protein aggregates' accumulation. For instance, a study focused on PD patients who developed dementia revealed that apart from α-seen accumulation in the neocortex, there was also was widespread Aβ accumulation in about 60% of the patients, with 3% of cases showing tau accumulation in addition to α-seen and Aβ[10]. Consequently, highly selective α-seen agents are desirable for an accurate diagnosis of PD.

The recent approval of several small-molecule Aβ positron emission tomography (PET) imaging agents has dramatically improved the enrichment of cohorts for Alzheimer's disease (AD) drug clinical trials[11] and invigorated the search for similar agents

against other proteinopathies [12,13,14]. A variety of molecular scaffolds (Fig. **1**) with moderate to high binding affinities to α-seen fibrils (albeit low selectivity versus Aβ fibrils, except **[^{18}F]WC-58a**) have been reported over the past decade as potential PET agents, but none have been successful in clinical translation[13,15-17]. The discovery of new molecular scaffolds are desirable to further the search for clinically translatable α-seen ligands. We report the design, synthesis, and *in vitro* evaluation of novel 1-indanone and 1,3-indandione derivatives with moderate to high binding affinities to α-seen fibrils. The lead candidates show greater than 10x selectivity for α-seen versus Aβ fibrils and avidly label all forms of α-seen aggregates in confirmed PD brain tissue.

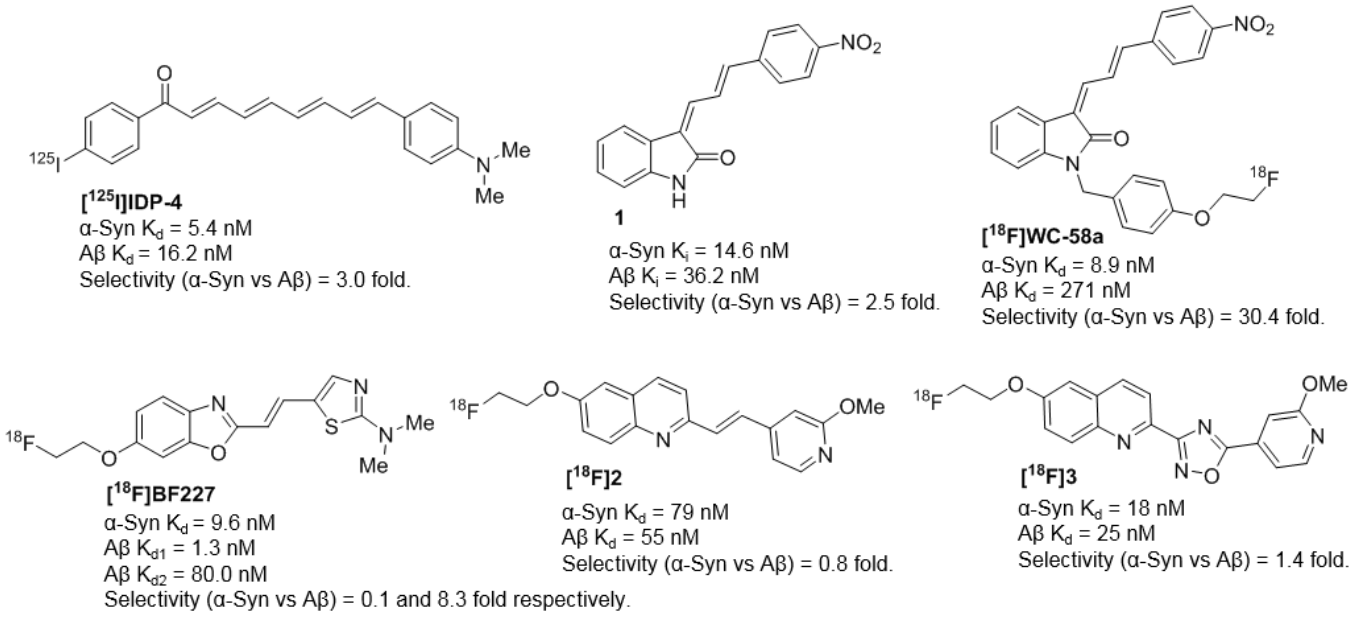

Figure **1**. Key representatives of α-synuclein aggregate binding ligands with some degree of selectivity versus Aβ aggregates.

2. Results and discussion

2.1. *Molecular design.*

A common feature in reported α-seen ligands is two aromatic ring systems separated by a spacer, which could be conjugated double bond(s) (compounds **[^{125}I]IDP-4**, **1**, **[^{18}F]WC-58a**, **[^{18}F]BF227,** and **[^{18}F]2**), or a heterocycle (**[^{18}F]3**). Structure-activity relationship studies (SAR) around **[^{125}I]IDP-4**[18], **1**, and **[^{18}F]WC-58a**[19,] respectively, suggested that the number and configuration of the conjugated double bonds play a significant role in both binding affinity and selectivity. For instance, in the indolinone series (1 and [18F]WC-58a), indolinone-dienes displayed higher binding affinities for both α-seen and Aβ fibrils over other indolinones[19]. Increase in steric bulk around compound **1** (α-Syn K_i = 14.6 nM and Aβ K_i = 36.2 nM) by replacing the N-H proton with a benzyl group in **[^{18}F]WC-58a** (α-Syn K_d = 8.9 nM and Aβ K_d = 271 nM) increased both binding affinity and selectivity for α-seen versus Aβ. Despite its high binding affinity and highest selectivity towards α-seen versus Aβ reported to date, the high *log P* value (4.18) of **[^{18}F]WC-58a** hampered further in vivo evaluation[19]. However, it provides a template for further SAR-based searches for small molecule ligands with high affinity and selectivity towards α-seen aggregates versus Aβ. Therefore, we chose compound **1** as a template for SAR studies in search of new small molecule constructs with high binding affinity and selectivity to α-seen aggregates.

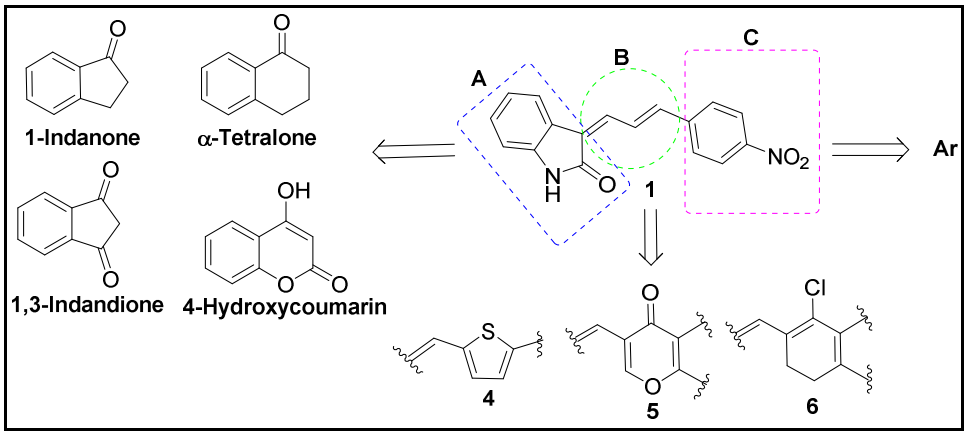

Figure **2**. Molecular design of new α-synuclein ligands.

Our molecular design (Fig. **2**) targeted all three parts of the molecule: the indolinone ring (**A**), the diene bridge (**B**), and the second aromatic ring (**C**). Previous reports suggest that a fused [6 + 5] ring system including 3- (benzylidene)-2-ones[19], the benzoxazole **[^{18}F]BF227**[20], the thiazole **[^{11}C]PBB3**[21,] and benzofuranones[22], for the "A" ring system may impart better affinity than a [6 + 6] ring system as observed with quinolines such as **[^{18}F]2** and **[^{18}F]3**. Furthermore, a α-carbonyl to the six-membered ring, as seen in the 3-(benzylidene)-2-ones and **[^{125}I]IDP-4**, also appears to contribute to the binding affinity. We, therefore, selected 1-indanone and 1,3-indandione as the starting points for new derivatives. α-Tetralone and 4-Hydroxycoumarin-based scaffolds were also included to verify further the observation that [6 + 5] ring systems are better binders than [6 + 6] ring systems for this portion of the molecule. For the bridging system, we maintained the diene in some derivatives, but also included derivatives in which one of the double bonds was replaced with an electron-rich thiophene moiety (**4**) to increase the electron density were also included. Derivatives with overall increased rigidity within the molecule were introduced by "locking" the second double bond in two different ring systems (**5** and **6**).

Derivatization around ring "**C**" employed both electron-rich and electron-deficient aromatic rings as well as heterocycles.

2.2. Chemical Synthesis.

As shown in Scheme **1**, the first series of derivatives (Fig. **3**) in which ring **A** is replaced with either a 1-indanon- (equation **i**, to generate compounds **7** – **15**), 1,3-indadion- (equation **ii**, to generate compounds **16** – **22**), α- teralonyl- (equation **iii**, to generate compounds **23** – **24**), or coumarin- (equation **iv**, to generate compounds **25**-**28**) moieties, while maintaining the diene bridge (**B**), were accessed by simple acid or base-catalyzed aldol condensation reactions of the desired keto substrate with the corresponding cinnamaldehyde derivatives. Early runs suggested that the monoketo substrates resulted in cleaner reaction products and better yields under acidic conditions while the diketo substrates preferred basic conditions. Therefore, subsequent reactions involving these substrates were carried out under similar reaction conditions. Both ^{1}H and ^{13}C NMR spectra of the resulting dienes showed peaks consistent with a single product, suggesting that only one of the two possible isomers (*E,E* or *Z,E*), was formed. Further analyses of their heteronuclear multiple bond connectivity (HMBC) and nuclear Overhauser effect (NOE) spectra suggested that the isolated products had the *E,E* configuration due to NOE enhancements observed between the highlighted protons (Fig. **4**).

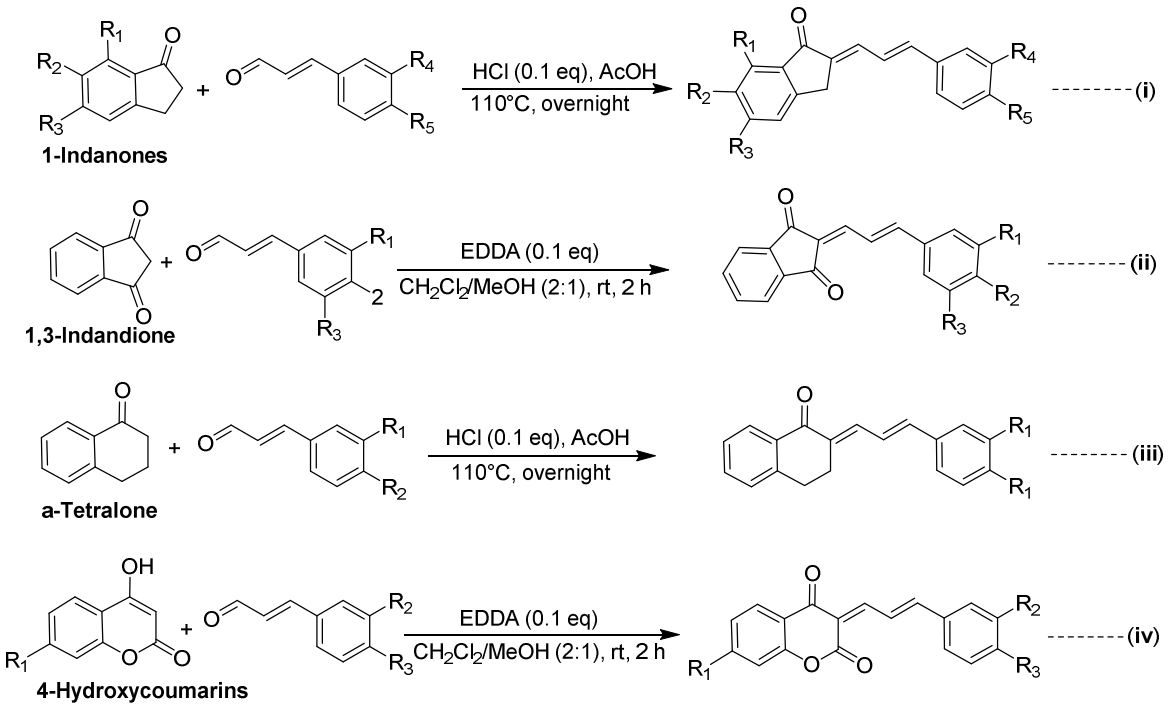

Scheme **1**. Synthetic routes to first generation 1-indanon-, 1,3-indandion-, α-tetralon-, and 4-oxocoumarin-diene derivatives.

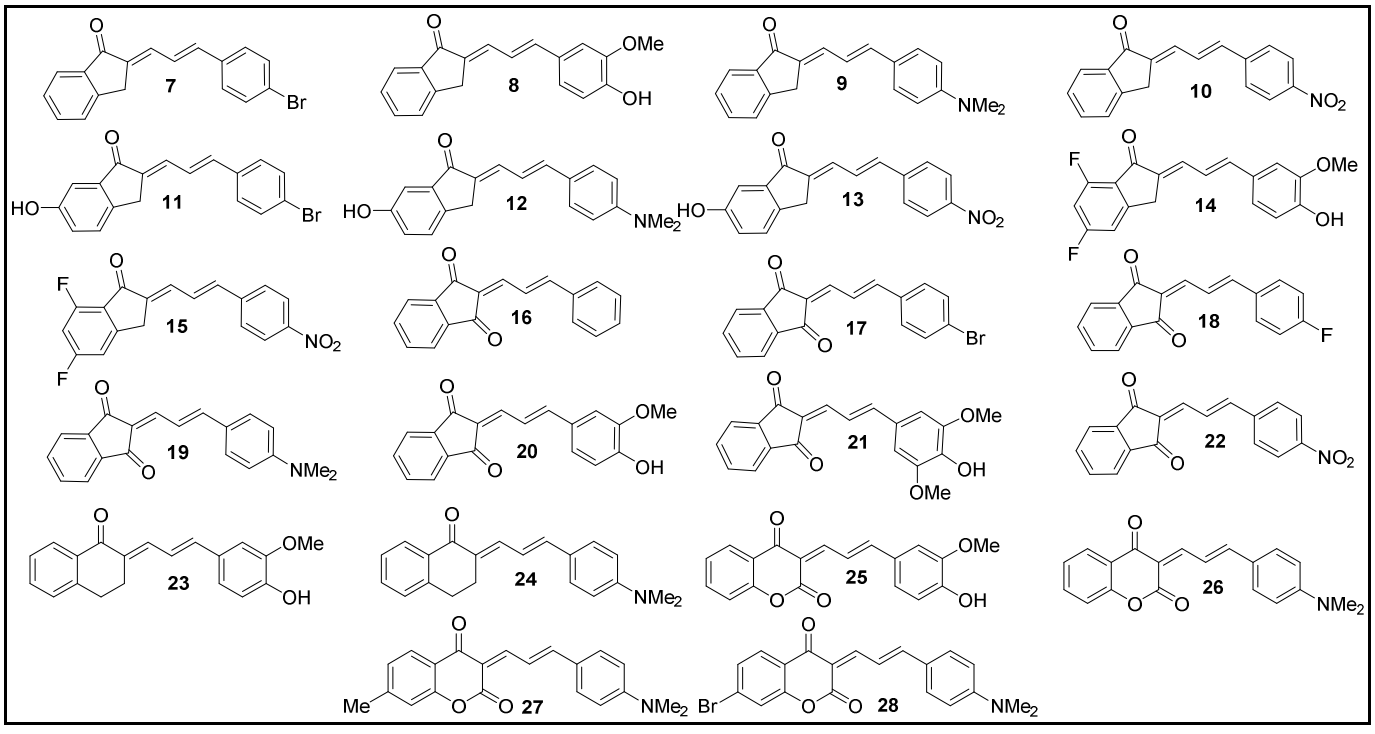

Figure **3**. First generation 1-indanon-, 1,3-indandion-, α-tetralon-, and 4-oxocoumarin-diene derivatives.

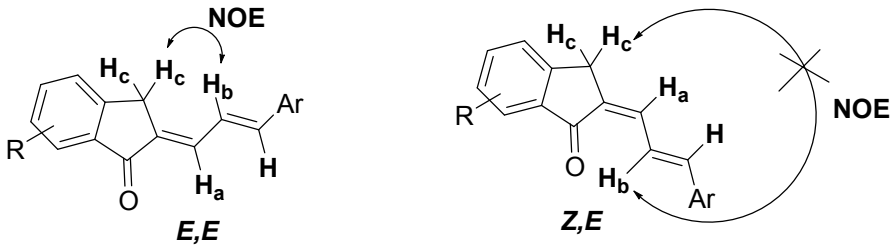

Figure **4**. Nuclear Overhauser effect in *E,E* configuration of diene derivatives.

The second series of 1-indanonyl- and 1,3-indandionnyl-diene derivatives (Fig. **5**) was generated by appending a second ring to 1-indanonyl-diene bromides (**7** and **11**), and 1,3-indandionnyl-diene bromide (**17**), via Suzuki coupling of the respective arylboronic esters to generate compounds **29**-**35** as shown in equations **v** and **vi** (Scheme **2**).

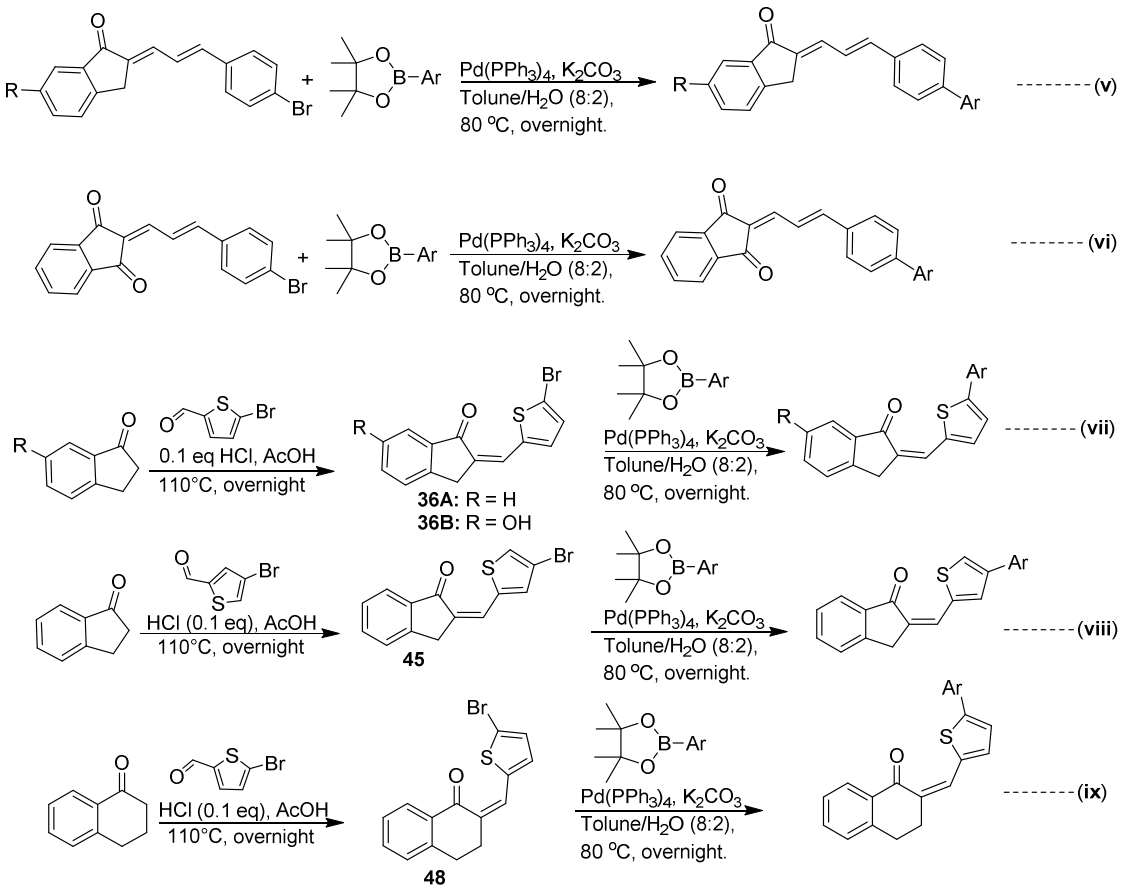

Scheme **2**. Synthetic routes to second-generation 1-indanon- and 1,3-indandion-diene derivatives with the second ring appended to ring to **C** and thiophene insertion into diene bridge.

Derivatives in which one of the double bonds of the bridging diene system is replaced with an electron-rich thiophene moiety to increase the electron density within the molecule were synthesized in two steps as shown in equations **vii - ix** (Scheme **2**). First, 5-bromo-2-thiophenecarboxaldehyde was exposed to 1-indanone (or 6-hydroxyl-1-indanone), under aldol condensation reaction conditions to yield the thiobromo intermediate **36**, which was then exposed to a variety of arylboronic esters under Suzuki coupling reaction conditions (equation **vii**) to generate compounds **37** - **44**. Similarly, other derivatives in this series were prepared from the aldol condensation of 1-indanone (equations **vii** and **viii**) and α-tetralone with 4-bromo-2-thiophenecarboxaldehyde and 5-bromo-2-thiophenecarboxaldehyde respectively, to generate the corresponding thiobromide intermediates **45** and **48**. These intermediates were then exposed to different arylboronic esters to obtain compounds **46** and **47**, and compounds **49** - **51,** respectively.

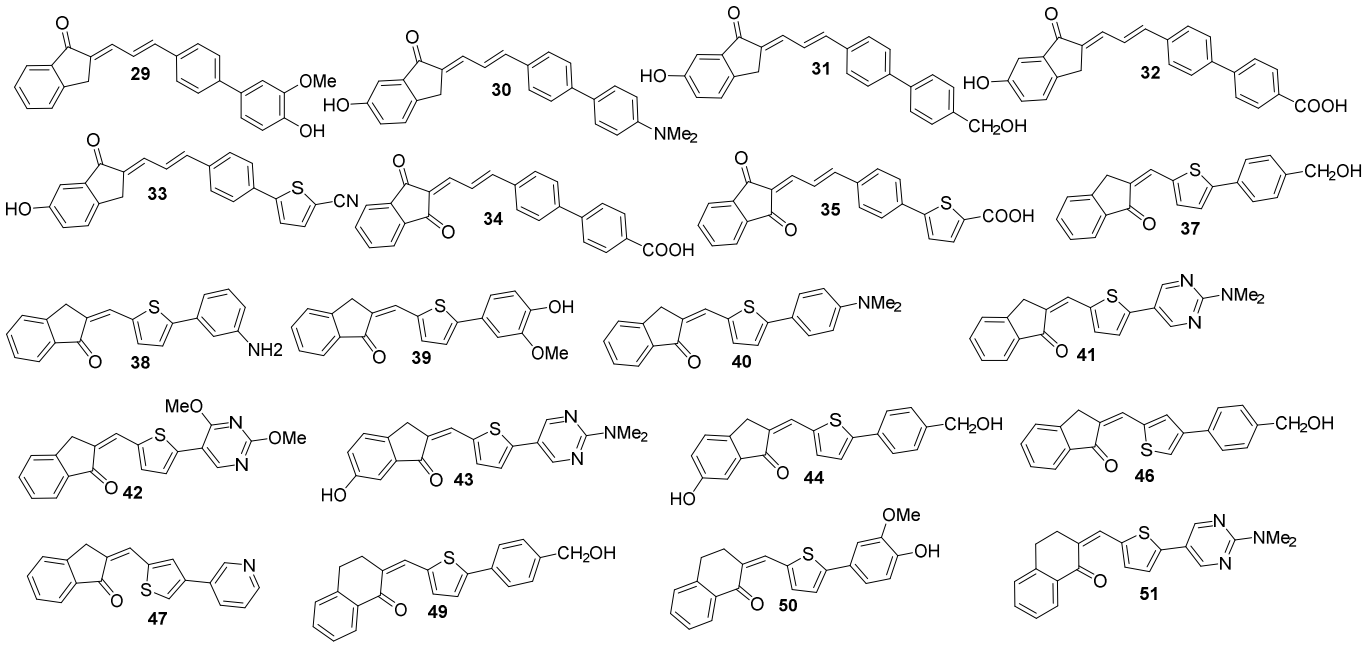

Figure **5**. Second generation 1-indanonyl- and 1,3-indandionnyl-diene derivatives with the second ring appended to ring to C and thiophene insertion into diene bridge.

Analysis of NOE (Fig. **6**) and HMBC spectra of compounds **36**, **45**, and **48** showed that the ensuing double bond from the respective aldol condensation reactions all had the *Z* conformation.

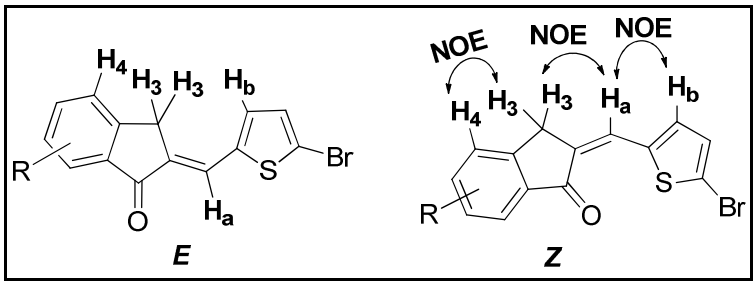

Figure **6**. NOE interactions in compounds **36**, **45**, and **48**.

Various derivatives (Fig. **7**) in which one of the double bonds of the bridging diene is masked within a ring system to increase rigidity within the molecule were accessed, as shown in Scheme **3**.

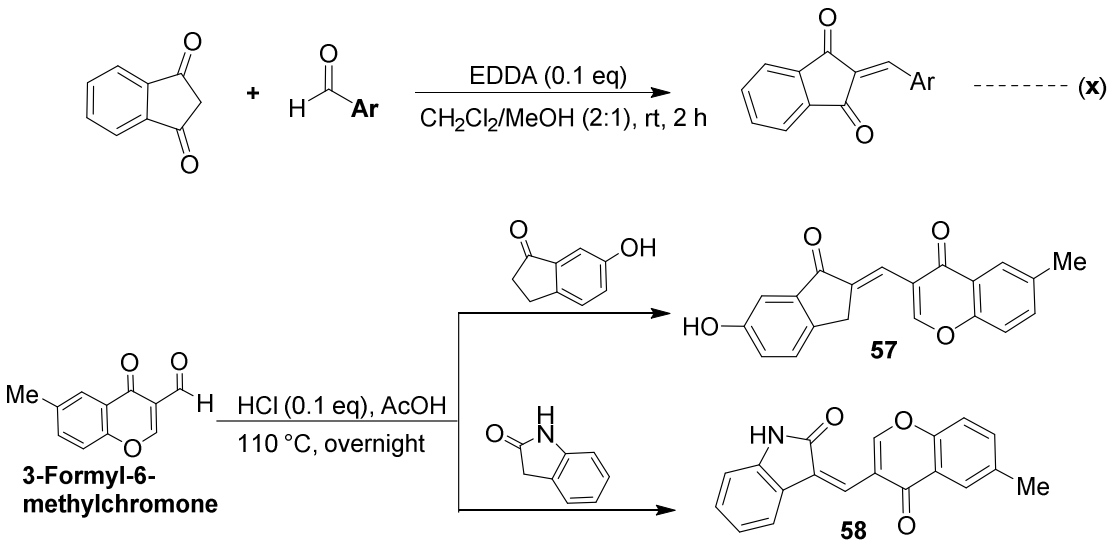

Scheme **3**. Synthesis of various derivatives with more rigid structures.

All members of this series were accessed in a single aldol condensation reaction between the respective keto-derivatives and corresponding aldehydes.

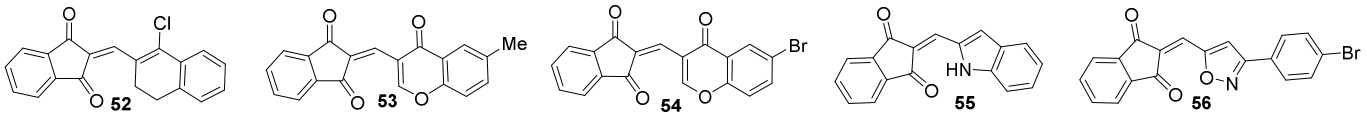

Figure **7**. Various derivatives.

Analysis of ^{1}H and ^{13}C NMR (see Supporting Information) and high-resolution mass spectra (HRMS) of each compound was used to elucidate each structure. UV/VIS

absorption and emission spectra of all compounds were recorded in phosphate-buffered saline (PBS), and those with fluorescence properties suitable for fluorescence microscopy studies were further evaluated in synthetic fibril binding studies.

2.3. Binding affinity (K_d) to synthetic α-syn fibrils.

All synthesized compounds (except **19** and **28**) exhibited fluorescence properties in PBS (Table **1**). To survey the relative binding affinity (K_d) of the ligands to α-syn fibrils, each ligand was subjected to a saturation binding protocol in which synthetic α-syn fibrils at a final concentration of 2.5 μM were incubated with increasing concentrations of the ligand for 1 hour. Specific binding was plotted against ligand concentration, and curve fitting to a one-site binding model using nonlinear regression in MATLAB software was used to establish saturation binding curves (See **S1** figures in Supporting Information). The reported relative K_d of each compound (Table 1) represents the mean K_d value determined by curve fitting the data to the equation $Y = B_{max} \times X/(X + K_d)$, from three different experiments, run in triplicates. All compounds with K_d values ≥ 2 μM (compounds **7**, **11**, **16**-**18**, **28**, **52**-**54**, and **56**) are reported as *no binding* (NB).

The 1-indanon-diene derivatives appeared to be better binders than the corresponding 1,3-indandion- diene, as exemplified by **8** vs. **20** and **10** vs. **22**. Any aromatic substitution (activating, **13** or deactivating, **14,** and **15**) on the 1-indanon-diene moiety reduces binding affinity compared to the non-substituted derivatives **10** and **8,**

respectively. The α-tetralon-diene and coumarin-diene derivatives all showed more inferior binding than the corresponding 1-indanon-diene and 1,3-indandion-diene derivatives, as exemplified by **8**, **20**, **23,** and **25**. Apart from compound **32** with a K_d of 18.8 ± 4.0 nM, appending a second ring to the phenyl group (**C**) does not appear to improve the binding affinity of either the 1-indanon-diene or 1,3-indandion-diene system. Similarly, replacing one of the double bonds in the diene bridge with an electron-rich thiopenyl moiety (compounds **8** vs. **39**) has no positive impact on the ligands' binding affinity to α-syn fibrils, albeit some modest K_ds (compounds **37** and **39**, and **42**). Rendering the system more rigid by masking the second double bond of the bridging diene in a fused ring with **C** (compounds **52** – **58**) leads to poor and non-binders.

Table **1**. Absorption/Emission maxima and binding affinity (K_d) of compounds to α-syn fibrils. K_d = mean ± SD (n = 3).

Compd.	*ID*	*Abs_{max}*	*Em_{max}*	*K_d α-syn (nM)*	*Log P[a]*	*Compd.*	*ID*	*Abs_{max}*	*Em_{max}*	*K_d α-syn (nM)*	*Log P[a]*
7	***XW-01-58***	332	430	NB	4.9	**32**	***XW-01-64***	392	563	18.8 ± 4.0	4.9
8	***XW-01-11***	405	542	9.0 ± 0.5	3.5	**33**	***XW-02-07***	398	565	148.7 ± 20.6	5.4
9	***XW-02-24***	450	589	38.4 ± 1.3	4.0	**34**	***XW-01-63***	358	409	1426 ± 46.8	4.4
10	***XW-01-09***	336	438	38.4 ± 1.3	3.6	**35**	***XW-01-60***	414	556	74.2 ± 14.3	4.4
11	***XW-01-52***	335	429	NB	4.5	**37**	***XW-01-92***	431	524	38.7 ± 4.1	4.6
12	***XW-01-61***	406	614	202.9 ± 15.9	3.9	**38**	***XW-02-16***	408	563	159.8 ± 10.0	4.4
13	***XW-01-16***	356	443	726.0 ± 23.6	3.3	**39**	***XW-02-17***	403	575	93.1 ± 13.8	4.1
14	***XW-01-18***	338	545	240.6 ± 47.9	3.8	**40**	***XW-02-14***	413	597	160.4 ± 7.1	5.5
15	***XW-01-17***	330	439	398.1 ± 3.9	3.9	**41**	***XW-01-84***	410	567	272.1 ± 29.9	4.1
16	***XW-01-53***	331	421	NB	3.1	**42**	***XW-02-15***	387	547	92.9 ± 6.3	4.3
17	***XW-01-50***	328	419	NB	3.9	**43**	***XW-01-83***	386	572	236.4 ± 10.4	3.7
18	***XW-01-01***	332	421	NB	3.3	**44**	***XW-02-01***	412	545	134.1 ±19.2	4.3
19	***XW-01-05***	416	--	NB	3.4	**46**	***XW-01-89***	368	454	153.3 ± 7.9	4.6
20	***XW-01-02***	402	572	44.5 ± 6.1	2.6	**47**	***XW-02-02***	340	404	333.1 ± 28.3	3.8
21	***XW-01-56***	434	450	268.2 ± 11.7	2.5	**49**	***XW-02-87***	372	551	161.6 ± 13.6	5.1
22	***XW-01-03***	336	460	1325.3 ± 181.8	2.8	**50**	***XW-02-88***	417	596	110.7 ± 7.8	5.1
23	***XW-02-21***	401	549	85.1 ± 13.4	3.9	**51**	***XW-02-89***	442	613	106.9 ± 7.5	4.5
24	***XW-02-22***	397	565	97.6 ± 5.7	4.7	**52**	***XW-01-29***	354	406	NB	2.7
25	***XW-02-90***	490	621	116.3 ± 0.7	2.9	**53**	***XW-01-28***	428	471	NB	2.3
26	***XW-01-45***	440	657	118.5 ± 21.1	3.7	**54**	***XW-01-27***	336	406	NB	3.9
27	***XW-01-46***	442	661	114.3 ± 13.5	4.2	**55**	***XW-01-31***	384	519	1183.1 ± 88.0	2.2

28	***XW-01-47***	405	--	NB	4.5	**56**	***XW-01-91***	321	409	NB	3.8
39	***XW-02-20***	397	551	66.7 ± 2.0	5.2	**57**	***XW-01-33***	326	388	655.6 ± 88.0	2.8
30	***XW-02-13***	414	597	236.3 ± 10.5	5.6	**58**	***XW-01-38***	344	385	1685.3 ± 252.0	2.4
31	***XW-01-87***	368	540	125.5 ± 5.0	4.7						

[a]*Obtained from ChemBioDraw Professional 16.*

2.4. Fluorescence properties and ligand binding to α-syn versus Aβ fibrils.

Although α-seen aggregates represent the most dominant misfolded protein aggregates encountered in PD and other synucleinopathies, several studies suggest that Aβ and tau aggregates often overlap with α-syn. For instance, in PD, α-syn accumulation may be accompanied by widespread accumulation of Aβ in a significant number of cases[10]. Potential α- syn agents for in vivo applications must be both highly sensitive and selective (especially versus Aβ) to minimize false positives in such cases. The preliminary α-syn fibril binding studies of 11 ligands showed high to moderate affinity ($K_d \leq 100$ nM). The fluorescence properties and binding affinity of these ligands to α-syn compared to Aβ fibrils were further evaluated. The absorption and emission maxima and the fluorescence quantum yields of the free ligand and in the presence of either α-syn or Aβ fibrils were determined. As exemplified by data for ligands **XW-01-11** and **XW-01-64** (Figure **8**), all the ligands show minimal fluorescence at concentrations ≤ 0.5 μM in aqueous media, but this increased remarkably upon the addition of either α-syn or Aβ fibrils.

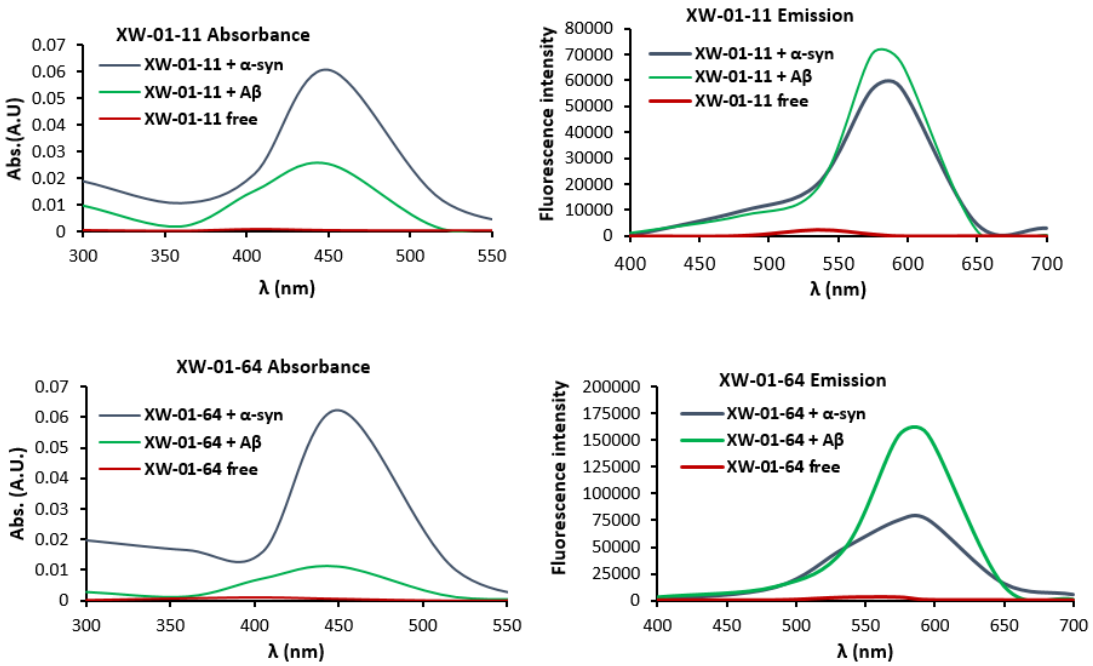

Figure 8. Samples of absorption/emission spectra of free ligands and when bound to α-syn or Aβ fibrils.

The increase in fluorescence is accompanied by a bathochromic shift in both absorbance and emission maxima from free molecule to ligand-fibril complex, accompanied by an 8 to 15 fold increase in fluorescence quantum yield upon ligand binding to α-seen fibrils and an additional 2 to 3 fold increase upon binding to Aβ fibrils (**Table 2**). Full details of the fluorescence properties, including fluorimetric titrations and quantum yield determination, are included in the supporting information (**S2**). The observed bathochromic shifts in fluorescence and emission maxima, the increase in fluorescence, and fluorescence quantum yields upon fibril binding by these ligands, are consistent with other observations of β-sheet binding ligands including the Thioflavin[23,24] and more recently reported benzofuranones[22].

Table 2. Fluorescent properties of ligand-fibril complexes of lead compounds.

		Abs_{max}		Em_{max}		Fluorescence quantum yield		
Compd.	ID	Ligand + α-sin	Ligand + Aβ	Ligand + α-sin	Ligand + Aβ	Free ligand	Ligand + α-sin	Ligand + Aβ
8	***XW-01-11***	446	441	585	579	0.0079	0.078	0.1363
9	***XW-02-24***	462	460	610	609	0.0059	0.0805	0.1465
20	***XW-01-02***	440	438	603	598	0.0061	0.0482	0.1419
23	***XW-02-21***	447	454	587	584	0.0051	0.0763	0.1890
24	**XW-02-22**	452	435	582	585	0.0063	0.0668	0.1377
29	***XW-02-20***	428	424	583	574	0.0052	0.0766	0.1543
32	***XW-01-64***	448	443	586	583	0.0104	0.1125	0.2498
34	**XW-01-60**	425	437	601	595	0.0097	0.0878	0.2058
37	***XW-01-92***	443	446	553	556	0.0063	0.0765	0.1074
39	***XW-02-17***	439	448	589	586	0.0031	0.0435	0.1377
42	***XW-02-15***	465	478	572	581	0.0050	0.0596	0.1130

The relative K_ds of the ligands binding to Aβ fibrils was determined in similar saturation binding assay with the α-syn fibrils. The results (Table **3**) suggest that in general, these ligands have a weaker affinity to Aβ compared to α-syn fibrils. Apart from compound **29**, all the other compounds have triple-digit Aβ fibril K_ds (nM), compared to double-digit α-syn fibril. A comparison between the two K_ds of each compound suggests that compound **8**, the lead α-seen binder (K_d α-syn = 9.0 ± 0.5 nM), has a 12.5 fold selectivity versus Aβ. The more moderate α-syn binders compounds **32** (K_d α-syn = 18.8 ± 4.0 nM) and **37** (K_d α-syn = 18.8 ± 4.0 nM) have 30.6 and 11.2 selectivity versus Aβ respectively. These double-digit selectivities make these the top three candidates from this study and are among the most selective α-syn versus Aβ ligands reported.

Table **3**. Comparison of α-syn versus Aβ fibril binding of top ligands. K_d = mean ± SD (n = 3).

Compd.	*ID*	*K_d α-syn (nM)*	*K_d Aβ (nM)*	*Selectivity α-syn v/s Aβ (fold)*
8	***XW-01-11***	9.7 ± 0.6	140.3 ± 4.2	14.4
9	***XW-02-24***	30.2 ± 4.0	156.7 ± 5.0	5.2
20	***XW-01-02***	38.5 ± 0.9	154.1 ± 11.8	4.0
23	***XW-02-21***	76.1 ± 23.4	143.7 ± 13.0	1.8
24	**XW-02-22**	94.8 ± 6.3	165.2 ± 7.1	1.7
29	***XW-02-20***	70.4 ± 9.6	52.5 ± 3.1	0.7
32	***XW-01-64***	18.8 ± 4.5	491.1 ± 58.9	26
34	**XW-01-60**	87.8 ± 16.8	337.3 ± 11.7	3.8
37	***XW-01-92***	34.9 ± 2.6	392.5 ± 64.4	11.2
39	***XW-02-17***	60.1 ± 32.8	256.7 ± 20.3	4.2
42	***XW-02-15***	91.2 ± 4.3	250.0 ± 37.1	2.7

The 1-indanone and 1,3-indadione derivatives reported herein were all synthesized in one or two steps employing facile aldol condensation and Suzuki coupling reactions, which are highly reproducible and scalable. The fibril binding experiments suggest that the 1-indanone and 1,3-indadione-dienes are better binders than the tetralones and coumarins. Apart from ligands **32** (K_d = 18.8 ± 4.0 nM) and **37** (K_d = 38.7 ± 4.1 nM) with moderate binding affinities, appending a second ring to ring C or replacing one of the double bonds in the diene bridge with a thiophene ring to increase electron density within the molecule does not appear to be favorable for binding. The top ten α-seen binders (except for **29**, K_d Aβ = 49.3 ± 4.9 nM) all show much lower affinity to Aβ fibrils suggesting a general selectivity for α-syn over Aβ aggregates by this structural class. The top two α-syn binders, **8** (K_d α-syn = 9.0 ± 0.5 nM) and **32** (K_d α-syn = 18.8 ± 4.0 nM) also turn out to be the most selective, with selectivity of 12.5 and 30.6x respectively. These K_d values and double-digit

selectivities are comparable to those of one of the highest binding and selective α-syn ligand [**^{18}F**]**WC-58a** (K_d α-syn = 8.9 nM and K_d Aβ = 271)[19], reported to date from fibril saturation binding assays. Taken together, our binding data, in combination with the recently reported benzofuranones[22], suggest that the [6+5] bicyclic ring system, **A** (Fig. **2**), is more favorable for binding and selectivity than a [6+6] system. As previously reported, the diene bridge, **B** (Fig. **2**) separating the two ring systems (**A** and **C**), appears essential. An increase in the system's electron density by replacing one of the double bonds with a thiophene ring does not appear to have any significant favorable impact on binding affinity or selectivity.

2.5. Fluorescent human PD and AD tissue staining.

The three lead ligands were further evaluated by *in vitro* fluorescent staining of neuropathologically verified postmortem brain samples from PD and AD cases. Two different anti-α-syn antibodies, Syn211[25], and Syn303[26], were employed to highlight misfolded α-syn aggregates in PD brain sections while the anti-Aβ antibody, 4G8, was used to highlight Aβ aggregates in the AD brain sections. The decision to use two different anti- α-syn antibodies is vital because while they both label misfolded α-syn aggregates, Syn211 is known to label all forms of aggregates including LBs and LNs as well as small thread and dot neurites (suggested to be markers of the very early stages of the disease), meanwhile Syn303 is more sensitive to mature LBs and LNs[26]. Sections from the PD brain's frontal-cortex were permeabilized and treated sequentially with antibody Syn211

and 1 μM solution of each compound and visualized by confocal microscopy. Figure **9**, column **I** (blue fluorescence), shows fluorescence HOECHST stain highlighting cell nuclei, thereby providing a perspective of cell bodies within the tissue. Column **II** (red) depicts ligand fluorescence, column **III** (green) depicts fluorescence from the antibody, and column **IV** is a composite image created by merging the first three images. Row **A** shows images obtained from a section of the frontal cortex from the PD brain, treated with compound **8** (**XW-01-11**). The ligand avidly labels Lewy pathology within the tissue. Colocalization of the ligand and antibody signals, with similar pattern and labeling intensity confirms that they both bind the same pathology.

Similarly, a section treated with ligand **32** (**XW-01-64**), row **B**, also shows the ligand's avid labeling of Lewy pathology by the ligand, which is corroborated by the staining pattern intensity of the antibody. As observed with ligand **8**, a composite image merging the ligand **32,** and the antibody images also show colocalization of both signals, confirming the efficiency of these ligands in labeling Lewy body pathology in postmortem human PD brain sections. In Z-stacked images of the treated tissue (Row **C**), the pathology appears to surround dark holes (white arrows) in the ligand and antibody channels. A composite image created by merging nuclear stain, ligand, and antibody signals shows that dark spots in the ligand and antibody channels are the spots occupied by the nuclei, which is more prominent at high magnification (**D**). The proximity and location of the nuclei suggest the presence of cytoplasmic inclusions.

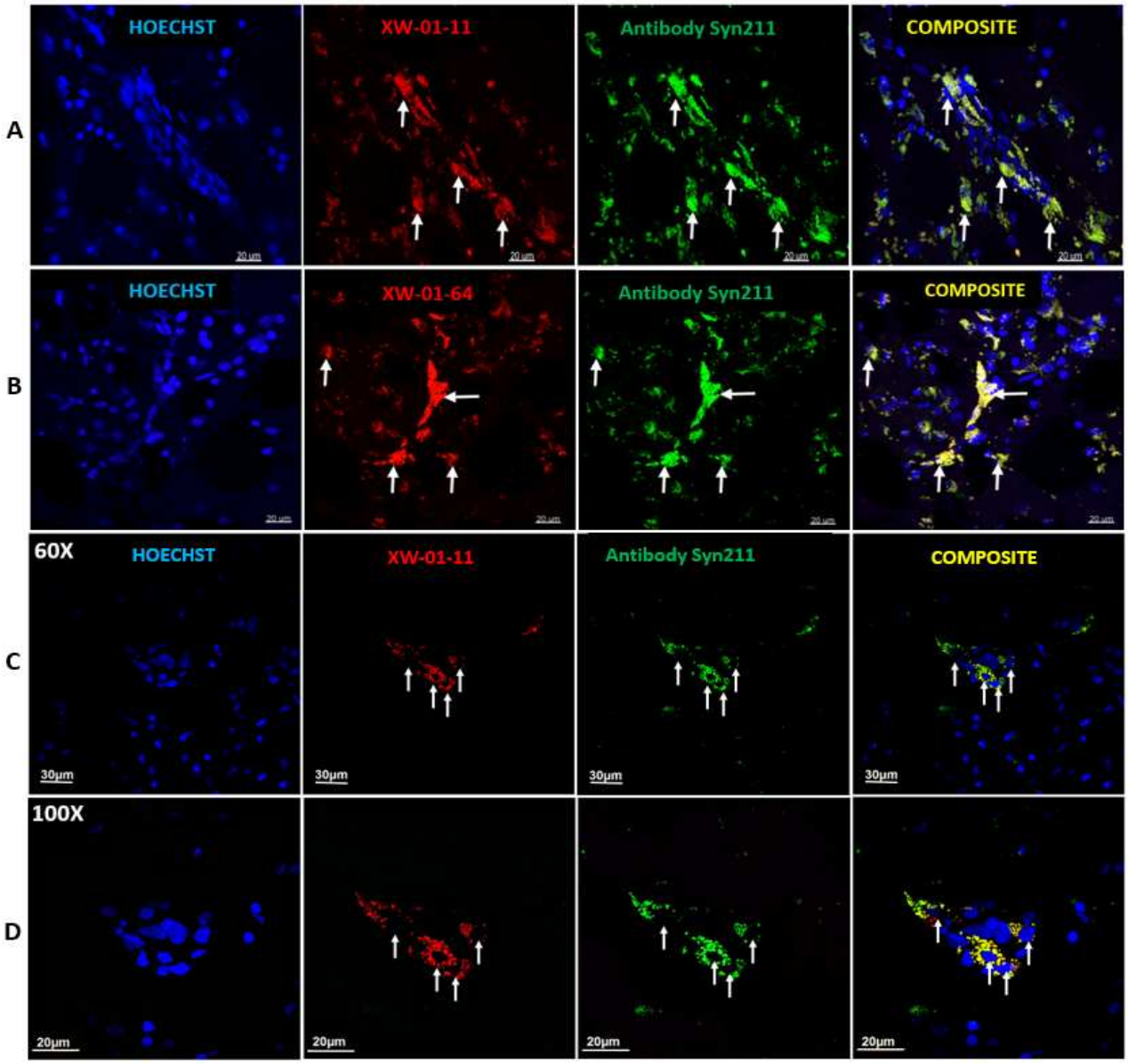

Figure 9. Confocal microscopy images of PD brain tissue sections co-stained with antibody, Syn211 and ligands **8** (**XW-01-11**) and **32** (**XW-01-64**) respectively. Fresh frozen brain sections were fixed with 10% formalin solution and then permeablized with 0.1% Triton-X 100. Section were incubated with antibody, followed by the respective ligands and HOECHST. **A**) Section of the frontal cortex treated with compound **8** (red) show avid labeling of Lewy pathology within the tissue. Labeling pattern is consistent in the antibody channel (green) and a composite of the two images shows colocalization of the ligand and antibody signals. **B**) Section treated with ligand **32** (red) also shows avid labeling of Lewy pathology which is corroborated by antibody staining (green). A composite image of the two shows co-localization of both signals. **C**) Z-stacked image of treated tissue the pathology appears to surround dark holes (white arrows) in the ligand and antibody channels. **D**) Composite images at higher magnification created by merging nuclei stain, ligand, and antibody signals show that dark spots in the ligand and antibody channels are the spots occupied by the nuclei, suggesting (as expected), that the observed pathology are cytoplasmic inclusions and not extracellular aggregates. Sample images from control brain tissue without any pathology are included in the Supporting Information (**S3**).

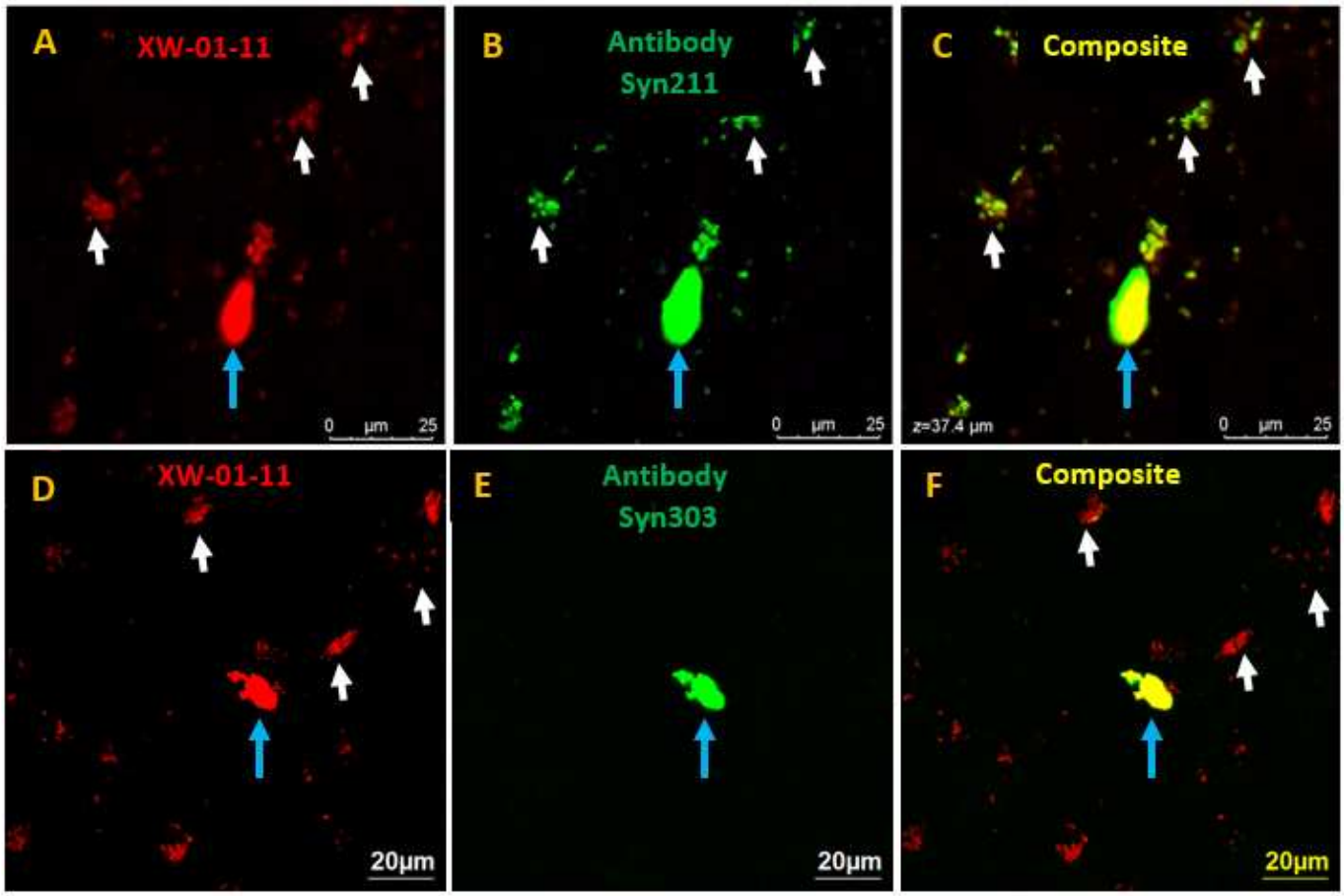

Figure 10. Confocal microscopy studies on contiguous PD brain sections show that ligands bind all conformations of α-seen aggregates including early stage small dot and thread neurites as well as mature Lewy bodies as exemplified by **XW-01-11**. **A**) Confocal microscopy images of PD brain section treated with ligand and antibody Syn211 which labels all forms of α-seen aggregates shows labeling of both early stage (white arrows) and mature Lewy pathology (blue arrow) in the ligand channel. **B**) Fluorescence due to antibody Syn211 staining shows a similar to ligand channel. **C**) Composite image from the ligand and Syn211 fluorescence shows colocalization of the two signals from both early stage and mature Lewy pathology. **D**) PD brain section treated with ligand and antibody Syn303 (which preferentially labels mature Lewy pathology) shows all forms of α-seen aggregates in the ligand channel. **E**) Fluorescence due to antibody Syn303 staining shows only the mature Lewy body. **F**) Composite image from the ligand and Syn303 fluorescence shows colocalization of the two signals only for the mature Lewy body.

To further characterize the sites labeled by labeled by the ligands and antibody Syn211 tissue staining experiments, were indeed α-seen, contiguous cortical section were treated with the lead ligand, and then either Syn211 or Syn303. As expected, the sections treated with the ligand and Syn211 (Fig. **10**, first row) show identical ligand and antibody labeling patterns that colocalize in the composite image. Both the ligand and antibody

appear to label all forms of pathology present on the tissue. On the other hand, tissue sections treated with the ligand and antibody Syn303 (Fig. **10**, second row) show effective labeling of both small neurites (white arrows) in the ligand channel but only mature Lewy bodies in the antibody channel (blue arrow). These findings suggest that the labeled pathology is α-syn and that the ligand labels all conformations of the pathology.

To assess the observed selectivity in α-seen versus Aβ fibril binding on aggregates on human tissue, equimolar concentrations of the top three lead candidates were further evaluated on PD tissue and cortical sections from neuropathologically-verified postmortem brain samples of AD cases. Figure **11** shows data from the top binder (**8**), demonstrating a 12.5-fold selectivity for α-seen vs. Aβ. As can be observed in Row **A**, the PD tissue shows the avid labeling of both large and fine pathology (column **II**). A similar labeling pattern and efficiency are also observed in the antibody channel (column **III**) and a composite image generated by merging both signals with the HOECHST signal (column **IV**) shows colocalization of the ligand and antibody signals. Unlike the PD tissue, fluorescent images from the AD tissue (Row **B**) show mostly dense core Aβ plaques in the ligand channel (column **II**) but not the finer aggregates composed of diffuse plaques. Amyloid pathology was clearly labeled by the 4G8 antibody (column **III**). A composite image generated by merging both signals with the HOECHST channel demonstrated an overlap of the ligand and 4G8 (column **IV**). High magnification images from the treated AD tissue (Row **C**)

show that, as expected, the observed Aβ pathology is extracellular, unlike the intracellular Lewy pathology observed in the PD tissue.

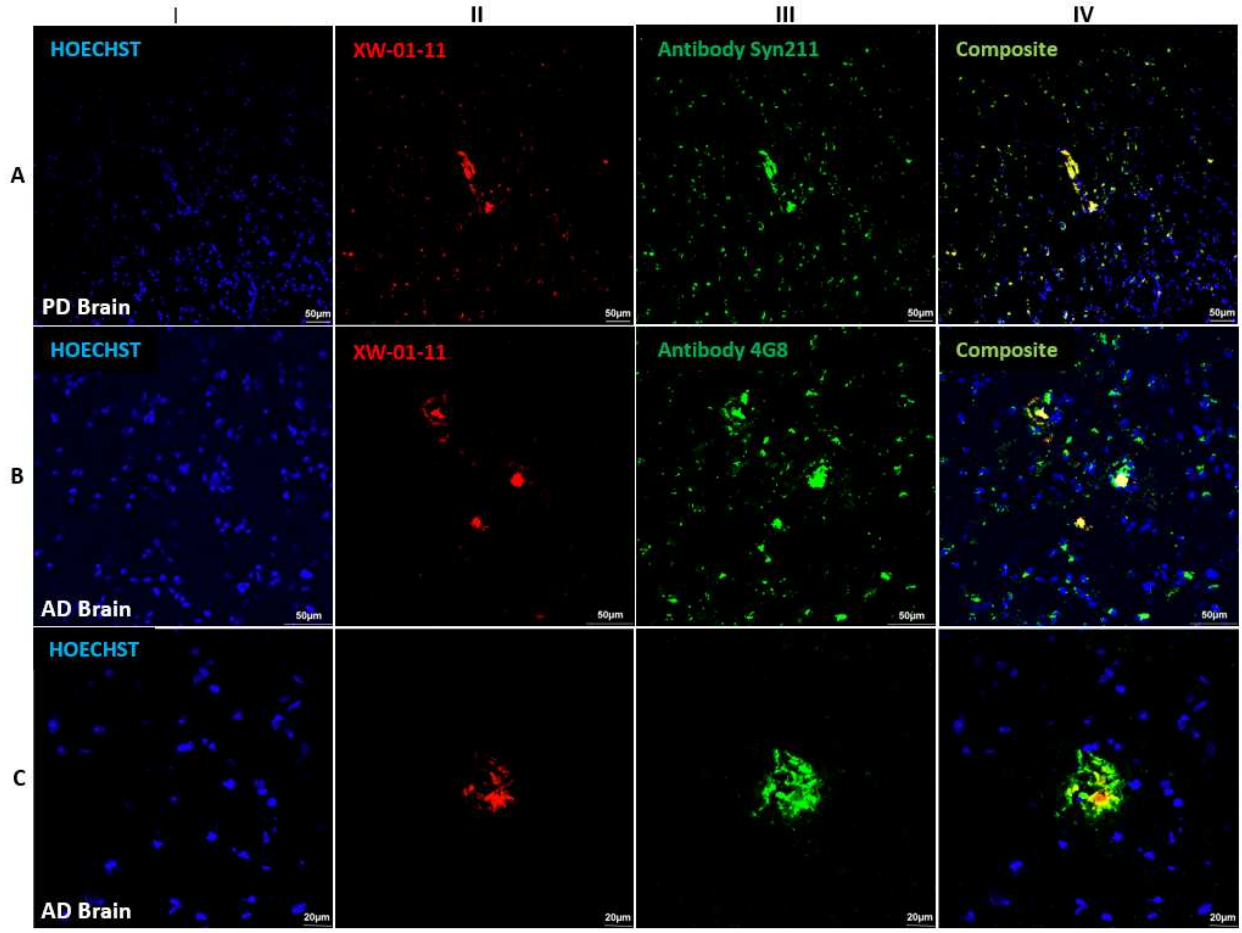

Figure 11. Comparative confocal microscopy images of PD and AD brain sections co-stained with **XW-01-11** and antibodies Syn211 and 4G8 respectively. **A**) Ligand (red) and antibody (green) avidly label both small and large deposits of α-seen pathology on PD tissue section. A composite image generated by merging the two images shows colocalization of both signals. **B**) Unlike the PD brain tissue, ligand (red) labeling on the AD tissue highlights mostly dense core Aβ plaques, while the antibody (green) labels the dense core plaques as well as diffuse and smaller Aβ aggregates. A composite image generated by merging both signals with the nuclear stain (blue) show overlap of the ligand signals from the dense core plaques suggesting that the ligand labels compact Aβstructures more efficiently than diffuse structures. **C**) Higher magnification images show that as expected, the observed pathology in the AD tissue sections is extracellular.

Quantification of the degree of colocalization between the ligand and the antibody signals in each tissue by ImarisColoc (Fig. **12**) results in a Pearson Correlation Coefficient (PCC) of 0.9 ligand-antibody signals in the PD tissue and 0.8 for signals in the AD tissue.

This data, combined with the fibril binding data, suggests that ligand binds fibrillar α-seen with greater efficiency than fibrillar Aβ.

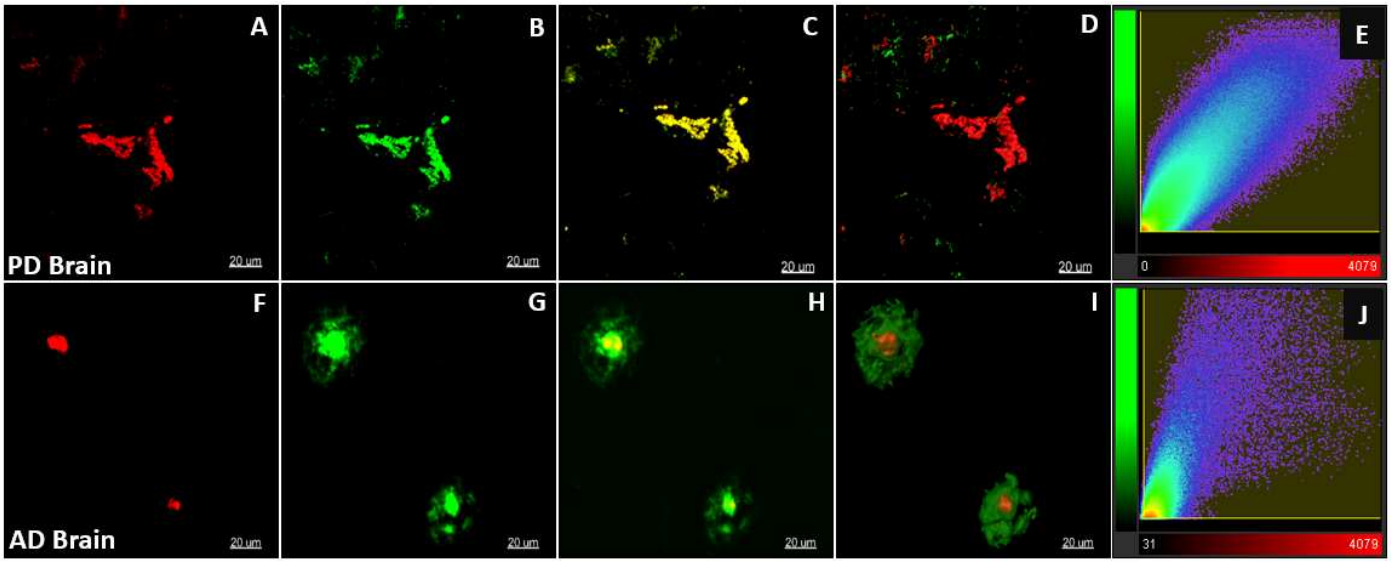

Figure 12. Colocalization analysis of the ligand and antibody signals. **A**) Fluorescence due to ligand staining of Lewy pathology in PD tissue; **B**) Fluorescence from antibody Syn211; **C**) Merged ligand and antibody signals; **D**) ImarisColoc 3D image of fluorescence intensities within the colocalized volume; **E**) Scatter plot of pixels within the colocalized volume shows a very slight deflection of the pixel distribution towards the green channel, resulting in a PCC of 0.9 from statistics over the entire volume; **F**) Red signal due to ligand staining of Aβ pathology in AD tissue; **G**) Fluorescence from antibody 4G8; **H**) Merged ligand and antibody signals; **I**) ImarisColoc 3D image of fluorescence intensities within the colocalized volume; **J**) Scatter plot of pixels within the AD tissue colocalized volume shows a higher deflection of the pixel distribution towards the green channel which results in a PCC of 0.8

3. Conclusion

This study demonstrated 1-indanone and 1,3-indadione derivatives as novel scaffolds for α-seen aggregates binding ligands. These were identified from a SAR study examining both the ring systems and bridging diene of the 3-(bezylidene)indolin-2-one diene scaffold,

the source of the most potent and selective α-syn ligands reported to date. All compounds were readily accessed via simple and readily scalable chemistries, and a majority of them possess adequate fluorescent properties in aqueous media, making them suitable for easy evaluation in biological systems. Saturation fibril binding studies suggest that the lead candidates have high binding affinities to α-syn aggregates and show significant selectivity towards these protein aggregates versus Aβ aggregates. Their potential as desirable ligands for applications in α-syn aggregates studies is further highlighted by the PD and AD brain tissue staining data, demonstrating that the ligands avidly bind all the different conformations of α-syn pathology present in both early and later stages of the disease.

4. Experimental

4.1. Chemical synthesis

4.1.1. General methods

All reagents were obtained from either Sigma-Aldrich, TCI, Alfa Aesar, or Acros Organics and used without further purification. Proton nuclear magnetic resonances (^{1}H NMR) were recorded at 600 MHz or 500 MHz on Bruker 600 or 500 NMR spectrometers. Carbon nuclear magnetic resonances (^{13}C NMR) were recorded at 75 MHz or 125 MHz on a Bruker 300 or 500 NMR spectrometers, respectively. Chemical shifts are reported in parts per million (ppm) from internal standards: acetone (2.05 ppm), chloroform (7.26 ppm), or dimethylsulfoxide (2.50 ppm) for ^{1}H NMR; and from an internal standard of

either residual acetone (206.26 ppm), chloroform (77.00 ppm), or dimethylsulfoxide (39.52 ppm) for ^{13}C NMR. NMR peak multiplicities are denoted as follows: s (singlet), d (doublet), t (triplet), q (quartet), dd (doublet of doublet), td (doublet of triplet), dt (triplet of doublet), and m (multiplet). Coupling constants (*J*) are given in hertz (Hz). High-resolution mass spectra (HRMS) were obtained from The Ohio State University Mass Spectrometry and Proteomics Facility. Thin-layer chromatography (TLC) was performed on silica gel 60 F254 plates from EMD Chemical Inc., and components were visualized by ultraviolet light (254 nm) and/or phosphomolybdic acid, 20 wt% solution in ethanol. SiliFlash silica gel (230–400 mesh) was used for all column chromatography. HPLC confirmed the purity of the lead compounds, and the data shows that each compound's purity is >95%.

4.1.2. Synthesis method 1

To a solution of aldehyde (1.0 eq) and 1-indanone (1.0 eq) in acetic acid (10 mL) was slowly added concentrated HCl (0.5 mL). The reaction mixture was stirred at 110 ^{o}C overnight and then cooled to room temperature. The cooled reaction mixture was poured into ice water and solid filtered and recrystallized in methanol.

4.1.3. Synthesis method 2

To a solution of aldehyde (1.0 eq) and 1,3-indandione (1.0 eq) in dichloromethane/methanol (1:2, 10 mL) was slowly added ethylenediamine

dihydrochloride (0.25 mmol). The reaction mixture was stirred at room temperature for 5 hours, and the resulting solid filtered out and recrystallized with methanol.

4.1.4. Synthesis method 3

A solution of the desired bromoindanone/indandione derivative (1.0 eq), bronic acid derivative (2.0 eq), K_2CO_3 (1.0 eq) in 1, 4 - dioxane/ H_2O (4:1, 10 mL) was deoxygenated by bubbling argon through for 20 minutes. To this was added $Pd(PPh_3)_4$ (0.1 eq) and argon bubbled through for a further 5 minutes, then stirred at 110 ^oC overnight. The reaction mixture was then cooled and diluted with water (5 mL) and the aqueous layer extracted with ethyl acetate. The combined organic layer was then washed with saturated $NaHCO_3$, rinsed with brine, dried over Na_2SO_4, and concentrated under reduced pressure. The ensuing residue was purified by column chromatography to obtain the desired compound.

(*E*)-2-((*E*)-3-(4-Bromophenyl)allylidene)-2,3-dihydro-1H-inden-1-one (**7**). Prepared by **Method 1** with 1-indanone (132 mg, 1.0 mmol) and *trans*-4-bromocinnamaldehyde (211 mg, 1.0 mmol) to afford compound **7** as a yellow solid (300 mg, 90% yield). ^1H NMR (600 MHz, $CDCl_3$) δ 7.87 (d, J = 7.8 Hz, 1H), 7.26 (td, J_1 = 1.2 Hz, J_2 = 7.2 Hz, 1H), 7.18 (d, J = 16.8 Hz, 1H), 7.50 – 7.48 (m, 2H), 7.41 (d, J = 10.8 Hz, 1H), 7.39 – 7.31 (m, 3H), 7.03 (dd, J_1 = 11.4 Hz, J_2 = 15.6 Hz, 1H), 6.96 (d, J = 15.6 Hz, 1H), 3.86 (s, 2H); ^{13}C NMR (150 MHz, $CDCl_3$) δ 193.6, 148.8, 140.4, 139.1, 136.6, 135.2, 134.5, 132.8, 132.0, 128.6, 127.6, 126.2, 124.9, 124.2, 123.2, 30.4. HRMS (ESI) *calcd* for $C_{18}H_{14}BrO$ $[M+H]^+$ 326.0223, found, 326.0220.

(*E*)-2-((*E*)-3-(4-Hydroxy-3-methoxyphenyl)allylidene)-2,3-dihydro-1H-inden-1-one (**8**). Prepared by **Method 1** with 1-indanone (250 mg, 1.89 mmol) and 4-hydroxy-3-methoycinnamaldehyde (337 mg, 1.89 mmol) to afford compound **8** as a red solid (436 mg, 79% yield). ^{1}H NMR (600 MHz, DMSO-*d*6) δ 9.52 (s, 1H), 7.74 (d, *J* = 7.8 Hz, 1H), 7.69 (td, *J*1 = 1.2 Hz, *J*2 = 7.2 Hz, 1H), 7.64 (d, *J* = 7.8 Hz, 1H), 7.47 (t, *J* = 7.2 Hz, 1H), 7.29 (dt, *J*1 = 1.8 Hz, *J*2 = 10.2 Hz, 1H), 7.28 (s, 1H), 7.13 (d, *J* = 15.6 Hz, 1H), 7.09 (dt, *J*1 = 10.2 Hz, *J*2 = 15.6 Hz, 1H), 7.06 (d, *J* = 8.4 Hz, 1H), 6.81 (d, *J* = 8.4 Hz, 1H), 3.93 (s, 2H), 3.86 (s, 3H); ^{13}C NMR (150 MHz, DMSO-*d*6) δ 192.9, 149.6, 148.9, 148.4, 143.3, 139.3, 135.1, 134.9, 134.2, 128.4, 127.9, 127.1, 123.7, 122.6, 122.5, 116.1, 111.0, 56.2, 30.7. HRMS (ESI) *calcd* for $C_{19}H_{17}O_3$ $[M+H]^+$ 293.1172, found, 293.1171.

(*E*)-2-((*E*)-3-(4-(Dimethylamino)phenyl)allylidene)-2,3-dihydro-1H-inden-1-one (**9**). Prepared by **Method 1** with 1-indanone (132 mg, 1.0 mmol) and 4-(dimethylamino)-cinnamaldehyde (175 mg, 1.0 mmol) to afford compound **9** as a dark red solid (200 mg, 69% yield). ^{1}H NMR (600 MHz, CDCl3) δ 7.86 (d, *J* = 7.8 Hz, 1H), 7.56 (td, *J*1 = 1.2 Hz, *J*2 = 7.8 Hz, 1H), 7.51 (d, *J* = 7.8 Hz, 1H), 7.44-7.38 (m, 4H), 6.97 (d, *J* = 15.0 Hz, 1H), 6.83 (dd, *J*1 = 12.0 Hz, *J*2 = 15.0 Hz, 1H), 6.66 (d, *J* = 9.0 Hz, 2H), 3.80 (s, 2H), 3.00 (s, 6H); ^{13}C NMR (150 MHz, CDCl3) δ 193.6, 151.1, 148.9, 143.2, 139.8, 134.9, 133.9, 133.4, 128.9, 127.4, 126.1, 124.5, 123.9, 119.8, 112.0, 40.2, 30.6. HRMS (ESI) *calcd* for $C_{20}H_{20}NO$ $[M+H]^+$ 290.1539, found, 290.1532.

(*E*)-2-((*E*)-3-(4-Nitrophenyl)allylidene)-2,3-dihydro-1H-inden-1-one (**10**). Prepared by **Method 1** with 1-indanone (150 mg, 1.1 mmol) and *trans*-4-

nitrocinnamaldehyde (200 mg, 1.1 mmol) to afford compound **10** as a yellow solid (300 mg, 85% yield). ^{1}H NMR (600 MHz, DMSO-*d*6) δ 8.26 (d, *J* = 10.8 Hz, 2H), 7.94 (d, *J* = 10.8, Hz, 2H), 7.76 (d, *J* = 9.0 Hz, 1H), 7.73 (t, *J* = 9.0 Hz, 1H), 7.66 (d, *J* = 9.0 Hz, 1H), 7.51 (dd, *J*1 = 13.2 Hz, *J*2 = 18.6 Hz, 1H), 7.47 (t, *J* = 9.0 Hz, 1H), 7.37 (d, *J* = 18.6 Hz, 1H), 7.32 (d, *J* = 13.2 Hz, 1H), 4.0 (s, 2H); ^{13}C NMR (150 MHz, DMSO-*d*6) δ 193.2, 149.9,147.5, 143.3, 139.4, 139.3, 138.8, 135.5, 132.2, 129.9, 128.8, 128.2, 127.2, 124.6, 124.0, 30.7. HRMS (ESI) *calcd* for $C_{18}H_{14}NO_3$ $[M+H]^+$ 292.0968, found, 292.0967.

(*E*)-2-((*E*)-3-(4-Bromophenyl)allylidene)-6-hydroxy-2,3-dihydro-1H-inden-1-one (11). Prepared by **Method 1** with 6-hydroxy-indanone (148 mg, 1.0 mmol) and *trans*-4-bromocinnamaldehyde (211 mg, 1.0 mmol) to afford compound **11** as a yellow solid (320 mg, 87% yield). ^{1}H NMR (600 MHz, DMSO-*d*6) δ 9.83 (s, 1H), 7.62 – 7.59 (m, 4H), 7.44 (d, *J* = 8.4 Hz, 1H), 7.26 (d, *J*1 = 11.4 Hz, *J*2 = 14.4 Hz, 1H), 7.23 – 7.21 (m, 1H), 7.18 (d, *J* = 14.4 Hz, 1H), 7.13 (dd, *J*1 = 2.4 Hz, *J*2 = 7.8 Hz, 1H), 7.04 (d, *J* = 2.4 Hz, 1H), 3.80 (s, 2H); ^{13}C NMR (150 MHz, DMSO-*d*6) δ 193.1, 157.6, 140.5, 140.2, 138.4, 136.0, 132.5, 132.3, 129.7, 127.9, 126.4, 123.7, 122.7, 108.5, 29.8. HRMS (ESI) *calcd* for $C_{18}H_{14}BrO_2$ $[M+H]^+$ 341.0172, found, 341.0169.

(*E*)-2-((*E*)-3-(4-(Dimethylamino)phenyl)allylidene)-6-hydroxy-2,3-dihydro-1H-inden-1-one (12). Prepared by **Method 1** with 6-hydroxy-indanone (148 mg, 1.0 mmol) and 4-(dimethylamino)-cinnamaldehyde (175 mg, 1.0 mmol) to afford compound **12** as a dark red solid (193 mg, 63% yield). ^{1}H NMR (500 MHz, DMSO-*d*6) δ 9.78 (s, 1H), 7.48 (d, *J* = 8.5 Hz, 2H), 7.43 (d, *J* = 8.0 Hz, 1H), 7.24 (d, *J* = 11.5 Hz, 1H), 7.13 – 7.05 (m,

2H), 7.03 (d, *J* = 2.0 Hz, 1H), 6.93 (dd, *J*1 = 11.5 Hz, *J*2 = 15.5 Hz, 1H), 6.72 (d, *J* = 9.0 Hz, 2H), 3.74 (s, 2H), 2.98 (s, 6H); ^{13}C NMR (125 MHz, DMSO-*d*6) δ 192.8, 157.5, 151.4, 143.4, 140.8, 140.2, 134.8, 134.4, 129.5, 127.8, 124.4, 123.1, 120.3, 112.4, 108.4, 39.1, 29.8. HRMS (ESI) *calcd* for $C_{20}H_{20}NO_2$ $[M+H]^+$ 306.1489, found, 306.1489.

(*E*)-6-Hydroxy-2-((*E*)-3-(4-nitrophenyl)allylidene)-2,3-dihydro-1H-inden-1-one (**13**). Prepared by **Method 1** with 6- hydroxy-indanone (148 mg, 1.0 mmol) and *trans*-4-nitrocinnamaldehyde (177 mg, 1.0 mmol) to afford compound **13** as a yellow solid (270 mg, 79% yield). ^{1}H NMR (600 MHz, DMSO-*d*6) δ 9.83 (s, 1H), 8.25 (d, *J* = 10.8 Hz, 2H), 7.92 (d, *J* = 10.8, Hz, 2H), 7.47 (d, *J* = 14.4 Hz, 1H), 7.45 (t, *J* = 6.0 Hz, 1H), 7.33 (d, *J* = 18.6 Hz, 1H), 7.26 (d, *J* = 13.8 Hz, 1H), 7.14 (dd, *J*1 = 3.0 Hz, *J*2 = 9.6 Hz, 1H), 7.05 (d, *J* = 3.0 Hz, 1H), 3.86 (s, 2H); ^{13}C NMR (150 MHz, DMSO-*d*6) δ 192.1, 156.6, 146.4, 142.2, 139.6, 139.2, 138.9, 138.1, 130.7, 128.9, 127.7, 126.9, 123.5, 122.9, 107.5, 28.8. HRMS (ESI) *calcd* for $C_{18}H_{14}NO_4$ $[M+H]^+$ 308.0917, found, 308.0916.

(*E*)-5,7-Difluoro-2-((*E*)-3-(4-hydroxy-3-methoxyphenyl)allylidene)-2,3-dihydro-1H-inden-1-one (**14**). Prepared by **Method 1** with 5,7-difluoro-1-indanone (200 mg, 1.2 mmol) and 4-hydroxy-3-methoycinnamaldehyde (212 mg, 1.2 mmol) to afford compound **14** as a black solid (320 mg, 81%). ^{1}H NMR (600 MHz, DMSO-*d*6) δ 9.53 (s, 1H), 7.33 (d, *J* = 9.0 Hz, 1H), 7.28-7.22 (m, 3H), 7.13 (d, *J* = 18.0 Hz, 1H), 7.06-7.00 (m, 2H), 3.95 (s, 2H), 3.85 (s, 3H); ^{13}C NMR (150 MHz, DMSO-*d*6) δ 188.4, 167.76 (d, *J* = 11.7 Hz), 165.74 (d, *J* = 11.4 Hz), 160.55 (d, *J* = 14.6 Hz), 158.47 (d, *J* = 14.5 Hz), 154.18 (d, *J* = 7.4 Hz), 149.1, 148.4, 143.9, 134.3, 134.2, 128.3, 123.6 (d, *J* = 13.2 Hz), 122.7, 122.2,

116.1, 110.9, 110.3 (d, J = 22.4 Hz), 104.1 (t, $J1$ = 23.8 Hz, $J2$ = 27.3), 56.2, 31.2. HRMS (ESI) *calcd* for $C_{19}H_{15}F_2O_3$ $[M + H]^+$ 329.0984, found, 329.0983.

(*E*)-5,7-Difluoro-2-((*E*)-3-(4-nitrophenyl)allylidene)-2,3-dihydro-1H-inden-1-one (**15**). Prepared by Method 1 with 5,7-difluoro-1-indanone (150 mg, 0.9 mmol) and *trans*-4-nitrocinnamaldehyde (158 mg, 0.9 mmol) to afford compound **15** as a yellow solid (251 mg, 83% yield). ^{1}H NMR (600 MHz, DMSO-$d6$) δ 8.26 (d, J = 8.4 Hz, 2H), 7.93 (d, J = 8.4, Hz, 2H), 7.48 (dd, J = 15.6, 5.4 Hz, 1H), 7.39-7.37 (m, 2H), 7.33-7.27 (m, 2H), 4.04 (s, 2H); ^{13}C NMR (150 MHz, CDCl3) δ 188.4, 167.6, 154.2, 154.1, 149.1, 148.4, 148.1, 143.9, 134.3, 128.3, 122.7, 122.2, 116.1, 111.0, 110.3 (d, J = 22.3 Hz), 104.1 (dd, $J1$ = 23.7 Hz, $J2$ = 26.8 Hz,), 56.2, 31.2. HRMS (ESI) *calcd* for $C_{18}H_{12}F_2NO_3$ $[M + H]^+$ 328.0780, found, 328.0779.

(*E*)-2-(3-Phenylallylidene)-1H-indene-1,3(2H)-dione (**16**). Prepared by **Method 2** with 1,3-indandione (146 mg, 1.0 mmol) and cinnamaldehyde (132 mg, 1.0 mmol) to afford compound **16** as a yellow solid (215 mg, 82% yield). ^{1}H NMR (600 MHz, CDCl3) δ 8.44 (dd, $J1$ = 15.6 Hz, $J2$ = 12.0 Hz, 1H), 7.97-7.95 (m, 2H), 7.78-7.76 (m, 2H), 7.66-7.65 (m, 2H), 7.80 (dd, $J1$ = 1.2 Hz, $J2$ = 12.0 Hz, 1H), 7.42-7.41 (m, 2H), 7.32 (d, J = 15.6 Hz, 1H); ^{13}C NMR (150 MHz, CDCl3) δ 190.4, 189.9, 151.0, 144.6, 142.1, 140.8, 135.5, 135.1, 134.9, 130.9, 128.9, 128.6, 127.9, 123.6, 123.1, 122.9. HRMS (ESI) *calcd* for $C_{18}H_{13}O_2$ $[M + H]^+$ 261.0910, found, 261.0912.

(*E*)-2-(3-(4-Bromophenyl)allylidene)-1H-indene-1,3(2H)-dione (**17**). Prepared by **Method 2** with 1,3-indandione (146 mg, 1.0 mmol) and *trans*-4-bromocinnamaldehyde

(211 mg, 1.0 mmol) to afford compound 17 as a yellow solid (300 mg, 86% yield). ^{1}H NMR (600 MHz, $CDCl_3$) δ 8.39 (dd, J_1 = 11.4 Hz, J_2 = 15.6 Hz, 1H), 7.95 (dt, J_1 = 2.4 Hz, J_2 = 5.46 Hz, 1H), 7.79 – 7.77 (m, 2H), 7.58 (d, J = 12.0 Hz, 1H), 7.55 – 7.51 (m, 2H), 7.50 (d, J = 8.4 Hz, 2H), 7.23 (d, J = 15.6 Hz, 1H); ^{13}C NMR (150 MHz, $CDCl_3$) δ 190.4, 189.9, 149.2, 143.9, 142.1, 140.8, 135.2, 135.1, 134.4, 132.2, 129.8, 128.3, 125.2, 124.1, 123.1, 122.9. HRMS (ESI) *calcd* for $C_{18}H_{12}BrO_2$ $[M + H]^+$ 339.0015, found, 339.0016.

(*E*)-2-(3-(4-Fluorophenyl)allylidene)-1H-indene-1,3(2H)-dione (**18**). Prepared by **Method 2** with 1,3-indandione (60 mg, 0.4 mmol) and trans-4-fluorocinnamaldehyde (62 mg, 0.4 mmol) to afford compound **18** as a yellow solid (100 mg, 88% yield). ^{1}H NMR (600 MHz, $CDCl_3$) δ 8.34 (dd, J_1 = 12.0 Hz, J_2 = 15.6 Hz, 1H), 7.96 – 7.94 (m, 2H), 7.79 – 7.76 (m, 2H), 7.64 (dd, J_1 = 6.6 Hz, J_2 = 8.4 Hz, 2H), 7.59 (d, J = 12.0 Hz, 1H), 7.26 (d, J = 15.6 Hz, 1H), 7.10 (t, J = 8.4 Hz, 2H); ^{13}C NMR (150 MHz, $CDCl_3$) δ 190.5, 189.9, 165.1, 163.4, 149.4, 144.3, 142.1, 140.8, 135.1 (d, J = 16.7 Hz), 131.8, 130.6 (d, J = 8.4 Hz), 127.9, 123.3, 123.14, 122.9, 116.3, 116.2 (d, J = 21.9 Hz). HRMS (ESI) *calcd* for $C_{18}H_{12}FO_2$ $[M + H]^+$ 279.0816, found, 279.0816.

(*E*)-2-(3-(4-(Dimethylamino)phenyl)allylidene)-1H-indene-1,3(2H)-dione (**19**). Prepared by **Method 2** with 1,3- indandione (146 mg, 1.0 mmol) and 4-(dimethylamino)-cinnamaldehyde (175 mg, 1.0 mmol) to afford compound **19** as a black solid (200 mg, 66% yield). ^{1}H NMR (600 MHz, $CDCl_3$) δ 8.23 (dd, J_1 = 12.0 Hz, J_2 = 15.6 Hz, 1H), 7.88 – 7.87 (m, 2H), 7.71 – 7.68 (m, 2H), 7.63 (dd, J_1 = 0.6 Hz, J_2 = 12.0 Hz, 1H), 7.56 (d, J =

8.4 Hz, 2H), 7.28 (d, *J* = 14.4 Hz, 1H), 6.69 (d, *J* = 9.0 Hz, 2H), 3.06 (s, 6H); ^{13}C NMR (150 MHz, $CDCl_3$) δ 191.2, 190.8, 153.7, 151.4, 146.5, 142.0, 140.7, 134.5, 134.3, 132.8, 131.4, 124.4, 122.6, 122.4, 119.3, 111.9, 40.2. HRMS (ESI) *calcd* for $C_{20}H_{18}NO_2$ $[M + H]^+$ 304.1332, found, 304.1332.

(*E*)-2-(3-(4-Hydroxy-3-methoxyphenyl)allylidene)-1H-indene-1,3(2H)-dione (**20**). Prepared by **Method 2** with 1,3- indandione (100 mg, 0.7 mmol) and 4-hydroxy-3-methoycinnamaldehyde (123 mg, 0.7 mmol) to afford compound **20** as a brown solid (201 mg, 96% yield). ^{1}H NMR (500 MHz, DMSO-*d*6) δ 10.04 (s, 1H), 8.16 (dd J_1 = 12.0 Hz, J_2 = 15.0 Hz, 1H), 7.90 (s, 4H), 7.65 (s, 1H), 7.62 (d, *J* = 5.0 Hz, 1H), 7.23 (s, 1H), 7.20 (d, *J* = 8.0 Hz, 1H), 6.91 (d, *J* = 8.0 Hz, 1H), 3.88 (s, 3H); ^{13}C NMR (125 MHz, DMSO-*d*6) δ 190.6, 189.9, 153.8, 151.3, 148.6, 145.5, 141.9, 140.6, 135.9, 135.8, 127.6, 125.9, 124.4, 123.1, 122.9, 120.5, 116.6, 112.0, 56.1. HRMS (ESI) *calcd* for $C_{19}H_{15}O_4$ $[M + H]^+$ 307.0965, found, 307.0962.

(*E*)-2-(3-(4-Hydroxy-3,5-dimethoxyphenyl)allylidene)-1H-indene-1,3(2H)-dione (**21**). Prepared by **Method 2** with 1,3-indandione (146 mg, 1.0 mmol) and *trans*-3,5-dimethoxy-4-hydroxycinnamaldehyde (208 mg, 1.0 mmol) to afford compound **21** as a yellow solid (290 mg, 81% yield). ^{1}H NMR (600 MHz, Acetone-*d*6) δ 8.36 (dd, J_1 = 12.0 Hz, J_2 = 15.6 Hz, 1H), 8.00 – 7.92 (m, 4H), 7.65 (d, *J* = 12.0 Hz, 1H), 7.60 (d, *J* = 15.6 Hz, 1H), 7.15 (s, 2H), 3.99 (s, 6H); ^{13}C NMR (150 MHz, DMSO-*d*6) δ 190.6, 189.9, 153.9, 148.7, 145.3, 141.9, 140.6, 140.5, 135.9, 135.8, 126.3, 126.0, 123.1, 122.9, 120.9, 107.0, 56.5. HRMS (ESI) *calcd* for $C_{20}H_{17}O_5$ $[M + H]^+$ 337.1071, found, 337.1070.

(*E*)-2-(3-(4-Nitrophenyl)allylidene)-1H-indene-1,3(2H)-dione (**22**). Prepared by **Method 2** with 1,3-indandione (100 mg, 0.7 mmol) and *trans*-4-nitrocinnamaldehyde (121 mg, 0.7 mmol) to afford compound **22** as a yellow solid (202 mg, 95% yield). ^{1}H NMR (600 MHz, CDCl3) δ 8.56 (dd, $J1$ = 12.0 Hz, $J2$ = 15.6 Hz, 1H), 8.28 (d, J = 9.0 Hz, 1H), 8.02-8.01 (m, 2H), 7.85-7.83 (m, 2H), 7.80 (d, J = 8.4 Hz, 1H), 7.63 (d, J = 12.0 Hz, 1H), 7.33 (d, J = 15.6 Hz, 1H); ^{13}C NMR (150 MHz, CDCl3) δ 190.2, 189.5, 148.5, 146.5, 142.4, 142.3, 141.5, 141.0, 135.6, 135.5, 130.1, 128.9, 127.3, 124.3, 123.4, 123.3. HRMS (ESI) *calcd* for $C_{18}H_{12}NO_4$ $[M + H]^+$ 306.0761, found, 306.0761.

(*E*)-2-((*E*)-3-(4-Hydroxy-3-methoxyphenyl)allylidene)-3,4-dihydronaphthalen-1(2H)-one (**23**). Prepared by **Method 2** with alpha-tetralone (146 mg, 1.0 mmol) and 4-hydroxy-3-methoxycinnamaldehyde (178 mg, 1.0 mmol) to afford compound **23** as a red solid (246 mg, 80% yield). ^{1}H NMR (600 MHz, CDCl3) δ 8.11 (d, J = 7.8 Hz, 1H), 7.56 (d, J = 10.8 Hz, 1H), 7.47 (t, J = 7.2 Hz, 1H), 7.35 (t, J = 7.2 Hz, 1H), 7.26 (d, J = 7.8 Hz, 1H), 7.08 (d, J = 7.8Hz, 1H), 7.03 – 6.94 (m, 3H), 6.92 (d, J = 8.4 Hz, 1H), 5.85 (s, 1H), 3.95 (s, 3H), 3.01 (s, 4H); ^{13}C NMR (150 MHz, CDCl3) δ 187.3, 146.9, 146.8, 143.4, 141.3, 136.5, 133.9, 133.3, 132.9, 129.4, 128.2, 128.1, 126.9, 121.5, 121.4, 114.8, 109.1, 56.0, 28.8, 25.9. HRMS (ESI) *calcd* for $C_{20}H_{19}O_3$ $[M + H]^+$ 307.1329, found, 307.1319.

(*E*)-2-((*E*)-3-(4-(Dimethylamino)phenyl)allylidene)-3,4-dihydronaphthalen-1(2H)-one (**24**). Prepared by **Method 2** with alpha-tetralone (146 mg, 1.0 mmol) and 4-(dimethylamino)-cinnamaldehyde (175 mg, 1.0 mmol) to afford compound **24** as a red solid (195 mg, 64% yield). ^{1}H NMR (600 MHz, CDCl3) δ 8.12 (d, J = 7.8 Hz, 1H), 7.61

(d, *J* = 10.2 Hz, 1H), 7.47 (t, *J* = 7.2 Hz, 1H), 7.43 (d, *J* = 8.4 Hz, 2H), 7.35 (t, *J* = 7.2 Hz, 1H), 7.25 (d, *J* = 7.8 Hz, 1H), 7.03 – 6.93 (m, 2H), 6.69 (d, *J* = 9.0 Hz, 2H), 3.03 (s, 6H), 3.01 (s, 4H); ^{13}C NMR (150 MHz, CDCl3) δ 187.3, 150.9, 143.4, 142.1, 137.6, 134.2, 132.7, 131.6, 128.7, 128.1, 128.0, 126.9, 124.9, 119.2, 112.1, 40.2, 28.8, 25.8. HRMS (ESI) *calcd* for $C_{21}H_{22}NO$ $[M + H]^+$ 304.1696, found, 304.1689.

3-(3-(4-Hydroxy-3-methoxyphenyl)allylidene)chromane-2,4-dione (**25**). Prepared by **Method 2** with 4-

hydroxycoumarin (162 mg, 1.0 mmol) and 4-hydroxy-3-methoycinnamaldehyde (178 mg, 1.0 mmol) to afford compound **25** as a black solid (187 mg, 58% yield). ^{1}H NMR (600 MHz, CDCl3) Major: δ 8.48 – 8.41 (m, 2H), 8.11 (d, *J* = 7.8 Hz, 1H), 7.65 – 7.61 (m, 1H), 7.54 (d, *J* = 13.8 Hz, 1H), 7.29 – 7.27 (m, 2H), 7.26 – 7.3 (m, 1H), 7.99 (d, *J* = 8.4 Hz, 2H), 6.15 (s, 1H), 4.01 (s, 3H); Minor: δ 8.75 (dd, *J*1 = 12.6 Hz, *J*2 = 15.0 Hz, 1H), 8.37 (d, *J* = 12.0 Hz, 1H), 8.07 (d, *J* = 7.2 Hz, 1H), 7.65 – 7.61 (m, 1H), 7.48 (d, *J* = 14.4 Hz, 1H), 7.29 – 7.27 (m, 1H), 7.26 – 7.3 (m, 1H), 7.02 – 7.0 (m, 1H), 6.94 (t, *J* = 7.2 Hz, 1H), 6.16 (s, 1H), 4.02 (s, 3H); ^{13}C NMR (150 MHz, DMSO-*d*6) δ Major:193.4, 144.5, 143.5, 143.2, 142.2, 140.6, 138.7, 135.9, 131.7, 128.4, 126.3, 125.9, 124.7, 124.6, 124.5, 123.7, 120.7, 58.5; Minor: 193.4, 144.9, 143.4, 142.2, 140.6, 138.4, 135.3,135.0, 131.6, 126.3, 126.3, 124.9, 124.7, 124.6, 124.4, 123.4, 120.7, 58.7. HRMS (ESI) *calcd* for $C_{19}H_{15}O_5$ $[M + H]^+$ 323.0914, found, 323.0908.

3-(3-(4-(Dimethylamino)phenyl)allylidene)chromane-2,4-dione (26). Prepared by **Method 2** with 4-

hydroxycoumarin (162 mg, 1.0 mmol) and 4-(dimethylamino)-cinnamaldehyde (175 mg, 1.0 mmol) to afford compound **26** as a blue solid (173 mg, 54% yield). ^{1}H NMR (600 MHz, DMSO-*d*6) Major: δ 8.37 (d, *J* = 12.6 Hz, 1H), 8.23 (d, *J* = 14.4 Hz, 1H), 7.99 (d, *J* = 14.4 Hz, 1H), 7.87 (d, *J* = 7.8 Hz, 1H), 7.72 – 7.70 (m, 2H), 7.65 (dd, *J*1 = 1.8 Hz, *J*2 = 7.8 Hz, 1H), 7.53 (t, *J* = 9.6 Hz, 1H), 6.89 (d, *J* = 9.0 Hz, 2H), 3.15 (s, 6H); Minor: δ 8.75 (dd, *J*1 = 12.6 Hz, *J*2 = 15.0 Hz, 1H), 6.89 (d, *J* = 9.0 Hz, 1H), 8.07 (d, *J* = 7.2 Hz, 1H), 7.65 – 7.61 (m, 1H), 7.48 (d, *J* = 14.4 Hz, 1H), 7.29 – 7.27 (m, 1H), 7.26 – 7.3 (m, 1H), 7.02 – 7.0 (m, 1H), 6.94 (t, *J* = 7.2 Hz, 1H), 6.16 (s, 1H), 4.02 (s, 3H); ^{13}C NMR (150 MHz, CDCl3 + DMSO-*d*6) δ Major: 180.2, 161.8, 161.1, 160.5, 154.9, 153.9, 135.1, 133.4, 126.8, 123.9, 123.5, 121.5, 120.1, 117.0, 113.3, 111.9, 39.9; Minor: 180.5, 164.5, 161.4, 161.1, 160.5, 154.9, 154.2, 134.8, 133.4, 126.5, 124.1, 123.4, 121.3, 120.1, 116.9, 112.0, 39.9. HRMS (ESI) *calcd* for $C_{20}H_{18}NO_3$ $[M + H]^+$ 320.1281, found, 320.1281.

3-(3-(4-(Dimethylamino)phenyl)allylidene)chromane-2,4-dione (**27**). Prepared by **Method 2** with 4-hydroxy-7- methylcoumarin (176 mg, 1.0 mmol) and 4-(dimethylamino)-cinnamaldehyde (175 mg, 1.0 mmol) to afford compound **27** as a blue solid (157 mg, 47% yield). ^{1}H NMR (600 MHz, DMSO-*d*6) Major: δ 8.37 (d, *J* = 12.6 Hz, 1H), 8.25-8.21 (m, 1H), 7.95 (d, *J* = 14.4 Hz, 1H), 7.75 (d, *J* = 9.6 Hz, 1H), 7.68 (d, *J* = 9.0 Hz, 2H), 7.53 – 7.50 (m, 1H), 7.20 (t, *J* = 8.4 Hz, 1H), 6.88 (t, *J* = 7.2 Hz, 2H), 3.14 (s, 6H), 2.37 (s, 3H); Minor: δ 8.65 (t, *J* = 13.8 Hz, 1H), 8.24-8.22 (m, 1H), 7.90 (d, *J* = 15.0 Hz, 1H), 7.75 (d, *J* = 9.6 Hz, 1H), 7.68 (d, *J* = 9.0 Hz, 2H), 7.53 – 7.50 (m, 1H), 7.20 (t, *J* = 8.4 Hz, 1H), 6.88 (t, *J* = 7.2 Hz, 2H), 3.14 (s, 6H), 2.38 (s, 3H); ^{13}C NMR (150

MHz, CDCl3 + DMSO-*d*6) δ Major: 180.3, 161.9, 161.3, 160.9, 153.6, 136.1, 133.7, 133.4, 126.4, 123.5, 121.5, 120.9, 119.6, 116.7, 113.3, 111.9, 39.9, 20.2; Minor: 180.6, 164.7, 161.1, 161.4, 160.5, 152.9, 135.7, 133.8, 133.3, 126.1, 123.3, 121.0, 120.8, 116.6, 113.2, 111.9, 39.9, 20.2. HRMS (ESI) *calcd* for $C_{21}H_{20}NO_3$ $[M + H]^+$ 334.1438, found, 334.1437.

6-Bromo-3-(3-(4-(dimethylamino)phenyl)allylidene)chromane-2,4-dione (**28**). Prepared by **Method 2** with 6-bromo-4-hydroxycoumarin (241 mg, 1.0 mmol) and 4-(dimethylamino)-cinnamaldehyde (175 mg, 1.0 mmol) to afford compound **28** as a blue solid (160 mg, 40% yield). ^{1}H NMR (600 MHz, DMSO-d_6) Major: δ 8.38 (d, *J* = 12.6 Hz, 1H), 8.23 (t, *J* = 14.4 Hz, 1H), 7.97-7.95 (m, 2H), 7.73-7.69 (m, 3H), 7.35 – 7.29 (m, 2H), 6.87-6.88 (m, 2H), 3.14 (s, 6H); Minor: δ 8.65 (t, *J* = 13.2 Hz, 1H), 8.23 (t, *J* = 14.4 Hz, 1H), 7.97-7.95 (m, 1H), 7.92 (d, *J* = 14.4 Hz, 1H), 7.73-7.69 (m, 3H), 7.35 – 7.29 (m, 2H), 6.87-6.88 (m, 2H), 3.14 (s, 6H); ^{13}C NMR (150 MHz, $CDCl_3$ + DMSO-*d*6) δ Major: 179.5, 161.1, 160.5, 154.9, 154.2, 153.2, 134.4, 132.7, 126.1, 123.3, 123.5, 122.8, 120.6, 119.4, 116.3, 112.6, 111.3, 39.2; Minor: 179.8, 163.8, 160.7, 159.7, 153.5, 153.2, 134.1, 132.7, 125.8, 123.4, 122.7, 120.6, 120.4, 116.2, 112.4, 111.3, 39.2. HRMS (ESI) *calcd* for $C_{20}H_{17}BrNO_3$ $[M + H]^+$ 398.0386, found, 398.0386.

(*E*)-2-((*E*)-3-(4'-Hydroxy-3'-methoxy-[1,1'-biphenyl]-4-yl)allylidene)-2,3-dihydro-1H-inden-1-one (**29**). Prepared by **Method 3** with compound **7** (160 mg, 0.5 mmol) and 4-hydroxy-3-methoxyphenylboronic acid pinacol ester (250 mg, 1.0 mmol) to afford compound **29** as a red solid (140 mg, 76% yield). ^{1}H NMR (600 MHz, $CDCl_3$) δ

7.87 (d, *J* = 7.8 Hz, 1H), 7.59 (t, *J* = 7.2 Hz, 1H), 7.55 (s, 4H), 7.52 (d, *J* = 7.8 Hz, 1H), 7.45 – 7.27 (m, 1H), 7.40 (d, *J* = 7.2 Hz, 1H), 7.40 (dd, $J1$ = 1.2 Hz, $J2$ = 7.8 Hz, 1H), 7.10 (s, 1H), 7.05 (d, *J* = 5.4 Hz, 2H), 7.00 (d, *J* = 7.8 Hz, 1H), 5.84 (s, 1H), 3.96 (s, 3H), 3.86 (s, 2H); ^{13}C NMR (150 MHz, $CDCl_3$) δ 193.7, 148.9, 146.9, 145.8, 141.9, 141.7, 139.3, 135.9, 134.8, 134.4, 133.6, 132.7, 127.8, 127.6, 127.1, 126.3, 124.2, 124.1, 120.2, 114.9, 109.5, 56.0, 30.5, 24.9. HRMS (ESI) *calcd* for $C_{25}H_{21}O_3$ $[M + H]^+$ 369.1486, found, 369.1474.

(*E*)-2-((*E*)-3-(4'-(Dimethylamino)-[1,1'-biphenyl]-4-yl)allylidene)-6-hydroxy-2,3-dihydro-1H-inden-1-one (30). Prepared by **Method 3** with compound **11** (170 mg, 0.5 mmol) and 4- (N,N-dimethylamino)phenylboronic acid pinacol ester (247 mg, 1.0 mmol) to afford compound **30** as a black solid (130 mg, 68% yield). ^{1}H NMR (600 MHz, DMSO-d_6) δ 7.76 (d, *J* = 7.8 Hz, 1H), 7.72-7.66 (m, 6H), 7.61 (d, *J* = 8.4 Hz, 2H), 7.49 (d, *J* = 7.2 Hz, 1H), 7.35 – 7.33 (m, 1H), 7.27 – 7.26 (m, 2H), 6.81 (d, *J* = 9.0 Hz, 2H), 3.98 (s, 2H), 2.97 (s, 6H); ^{13}C NMR (150 MHz, $CDCl3$ + DMSO-d_6) δ 194.4, 150.1, 149.0, 142.5, 141.9, 138.9, 135.2, 134.5, 134.3, 133.7, 127.7, 127.4, 127.2, 126.0, 123.8, 123.1, 112.6, 40.1, 30.2. HRMS (ESI) *calcd* for $C_{26}H_{24}NO$ $[M + H]^+$ 382.1802, found, 382.1808.

(*E*)-6-Hydroxy-2-((*E*)-3-(4'-(hydroxymethyl)-[1,1'-biphenyl]-4-yl)allylidene)-2,3-dihydro-1H-inden-1-one (**31**). Prepared by **Method 3** with compound **11** (170 mg, 0.5 mmol) and 4-(hydroxymethyl)phenylboronic acid pinacol ester (234 mg, 1.0 mmol) to afford compound **31** as a brown solid (129 mg, 70% yield). ^{1}H NMR (500 MHz, DMSO-d_6) δ 9.86 (s, 1H), 7.76 – 7.72 (m, 4H), 7.70 (d, *J* = 8.0 Hz, 2H), 7.46 (d, *J* = 8.0 Hz, 1H),

7.42 (d, *J* = 8.5 Hz, 2H), 7.29 – 7.26 (m, 3H), 7.13 (dd, $J1$ = 2.5 Hz, $J2$ = 8.0 Hz, 1H), 7.05 (d, *J* = 3.0 Hz, 1H), 5.24 (s, 1H), 4.55 (s, 2H), 3.83 (s, 2H); ^{13}C NMR (125 MHz, DMSO-d_6) δ 192.1, 141.7, 140.6, 140.0, 139.4, 139.3, 137.1, 136.9, 134.8, 131.9, 127.5, 126.9, 126.5, 126.4, 125.8, 124.5, 122.8, 107.5, 62.1, 28.8. HRMS (ESI) *calcd* for $C_{25}H_{21}O_3$ $[M + Na]^+$ 369.1485, found, 369.1480.

4'-((*E*)-3-((*E*)-6-Hydroxy-1-oxo-1,3-dihydro-2H-inden-2-ylidene)prop-1-en-1-yl)-[1,1'-biphenyl]-4-carboxylic acid (**32**). Prepared by **Method 3** with compound **11** (170 mg, 0.5 mmol) and 4-carboxyphenylboronic acid (166 mg, 1.0 mmol) to afford compound **32** as a gray solid (111 mg, 58% yield). ^{1}H NMR (600 MHz, DMSO-d_6) δ 13.20 (s, 1H), 7.81 (d, *J* = 7.8 Hz, 2H), 7.77 – 7.73 (m, 4H), 7.71 (t, *J* = 7.8 Hz, 1H), 7.7-7.65 (m, 3H), 7.48 (t, *J* = 7.8 Hz, 1H), 7.34 (d, *J* = 13.2 Hz, 2H), 7.27 (d, *J* = 13.8 Hz, 1H), 3.98 (s, 2H); ^{13}C NMR (150 MHz, DMSO-d_6) δ 193.1, 163.3, 149.8, 149.4, 141.4, 139.0, 137.3, 137.1, 135.2, 134.8, 133.8, 133.1, 128.8, 128.1, 127.2, 126.7, 126.2, 125.5, 123.9, 30.7. HRMS (ESI) *calcd* for $C_{25}H_{19}O_4$ $[M + H]^+$ 383.1278, found, 383.1277.

5-(4-((*E*)-3-((*E*)-6-Hydroxy-1-oxo-1,3-dihydro-2H-inden-2-ylidene)prop-1-en-1-yl)phenyl)thiophene-2- carbonitrile (**33**). Prepared by **Method 3** with compound **11** (170 mg, 0.5 mmol) and 5-cyanothiophene-2-boronic acid pinacol ester (235 mg, 1.0 mmol) to afford compound **33** as a red solid (131 mg, 71% yield). ^{1}H NMR (600 MHz, DMSO-d_6) δ 8.01 (d, *J* = 4.8 Hz, 1H), 7.82 (d, *J* = 10.2 Hz, 2H), 7.78 – 7.74 (m, 3H), 7.71 (t, *J* = 9.0 Hz, 1H), 7.65 (d, *J* = 9.0 Hz, 1H), 7.48 (t, *J* = 9.0 Hz, 1H), 7.38 – 7.25 (m, 3H), 3.97 (s, 2H); ^{13}C NMR (150 MHz, DMSO-d_6) δ 192.0, 149.9, 148.7, 140.1, 139.8, 137.9, 136.8,

136.5, 134.2, 131.9, 131.4, 127.8, 127.0, 126.1, 126.0, 125.9, 124.4, 122.8, 113.8, 106.3, 29.6. HRMS (ESI) *calcd* for $C_{23}H_{16}NOS$ $[M + H]^+$ 370.0896, found, 370.0896.

(*E*)-4'-(3-(1,3-Dioxo-1,3-dihydro-2H-inden-2-ylidene)prop-1-en-1-yl)-[1,1'-biphenyl]-4-carboxylic acid (**34**). Prepared by **Method 3** with compound **17** (170 mg, 0.5 mmol) and 4-carboxyphenylboronic acid (166 mg, 1.0 mmol) to afford compound **34** as a gray solid (120 mg, 68%). ^{1}H NMR (600 MHz, DMSO-d_6) δ 13.04 (s, 1H), 8.38 (dd, $J1$ = 12.0 Hz, $J2$ = 15.6 Hz, 1H), 8.05 (d, J = 8.4 Hz, 2H), 7.95-7.94 (m, 4H), 7.91 – 7.86 (m, 4H), 7.82 (d, J = 7.8 Hz, 2H), 7.79 (d, J = 15.6 Hz, 1H), 7.71 (d, J = 12.0 Hz, 1H); ^{13}C NMR (150 MHz, DMSO-d_6) δ 190.8, 190.0, 167.8, 151.5, 144.5, 143.9, 142.4, 141.9, 141.1, 136.6, 136.0, 134.9, 130.9, 130.8, 129.9, 128.6, 127.7, 124.0, 123.7, 123.6. HRMS (ESI) *calcd* for $C_{25}H_{17}O_4$ $[M + H]^+$ 381.1121, found, 381.1121.

(*E*)-5-(4-(3-(1,3-Dioxo-1,3-dihydro-2H-inden-2-ylidene)prop-1-en-1-yl)phenyl)thiophene-2-carboxylic acid (**35**). Prepared by **Method 3** with compound **17** (170 mg, 0.5 mmol) and 5-carboxythiophene-2-boronic acid pinacol ester (254 mg, 1.0 mmol) to afford compound **35** as a red solid (137 mg, 71% yield). ^{1}H NMR (600 MHz, DMSO-d_6) δ 8.36 (dd, $J1$ = 12.0 Hz, $J2$ = 15.6 Hz, 1H), 7.95 – 7.96 (m, 4H), 7.88 (d, J = 7.8 Hz, 2H), 7.77 (d, J = 7.8 Hz, 2H), 7.75 – 7.69 (m, 4H); ^{13}C NMR (150 MHz, DMSO-d_6) δ 190.5, 189.7, 169.8, 151.0, 150.9, 144.8, 144.1, 143.5, 142.1, 140.8, 137.4, 136.3, 134.3, 129.8, 128.2, 126.9, 126.3, 126.2, 126.1, 123.8, 123.7, 123.4, 123.2. HRMS (ESI) *calcd* for $C_{23}H_{15}O_4S$ $[M + H]^+$ 387.0686, found, 387.0686.

(*Z*)-2-((5-Bromothiophen-2-yl)methylene)-2,3-dihydro-1H-inden-1-one (**36A**). Prepared by **Method 1** with 1- indanone (650 mg, 5.0 mmol) and 5-bromo-2-thiophenecarboxaldehyde (1.43 g, 7.5 mmol) to afford intermediate **36A** as a yellow solid (1.5 g, 93% yield). ^{1}H NMR (600 MHz, DMSO-d_6) δ 7.30 (d, J = 7.8 Hz, 1H), 7.27 (dt, $J1$ = 1.2 Hz, $J2$ = 3.0 Hz, 1H), 7.25 (dd, $J1$ = 1.2 Hz, $J2$ = 7.2 Hz, 1H), 7.24 (dd, $J1$ = 0.6 Hz, $J2$ = 7.2 Hz, 1H), 7.07 (d, J = 4.2 Hz, 1H), 7.02 (td, $J1$ = 1.2 Hz, $J2$ = 7.8 Hz, 1H), 6.94 (d, J = 4.2 Hz, 1H), 3.44 (d, J = 1.2 Hz, 2H); ^{13}C NMR (150 MHz, DMSO-d_6) δ 193.0, 149.6, 141.5, 138.1, 135.4, 135.1, 133.7, 132.3, 128.2, 127.3, 125.5, 123.9, 117.9, 32.1. HRMS (ESI) *calcd* for $C_{14}H_{10}BrOS$ $[M + H]^+$ 304.9630, found, 304.9627.

(*Z*)-2-((5-Bromothiophen-2-yl)methylene)-6-hydroxy-2,3-dihydro-1H-inden-1-one (**36B**). Prepared by **Method 1** with 6-hydroxy-indanone (740 mg, 5.0 mmol) and 5-bromo-2-thiophenecarboxaldehyde (1.4 g, 7.5 mmol) to afford intermediate 36B as a yellow solid (1.4 g, 85% yield). ^{1}H NMR (600 MHz, DMSO-d_6) δ 9.86 (s, 1H), 7.67 (dd, $J1$ = 1.8 Hz, $J2$ = 2.4 Hz, 1H), 7.52 – 7.49 (m, 1H), 7.49 – 7.46 (m, 1H), 7.38 (d, J = 4.2 Hz, 1H), 7.13 (dd, $J1$ = 2.4 Hz, $J2$ = 8.4 Hz, 1H), 7.05 (d, J = 2.4 Hz, 1H), 3.75 (d, J = 1.8 Hz, 2H); ^{13}C NMR (150 MHz, DMSO-d_6) δ 193.0, 157.7, 141.5, 140.3, 139.4, 134.9, 134.8, 132.2, 128.0, 125.2, 123.9, 117.8, 108.6, 31.4. HRMS (ESI) *calcd* for $C_{14}H_{10}BrO_2S$ $[M + H]^+$ 320.9579, found, 320.9577.

(*Z*)-2-((5-(4-(Hydroxymethyl)phenyl)thiophen-2-yl)methylene)-2,3-dihydro-1H-inden-1-one (**37**). Prepared by **Method 3** with intermediate **36A** (152 mg, 0.5 mmol) and 4-(hydroxymethyl)phenylboronic acid pinacol ester (234 mg, 1.0 mmol) to afford

compound **37** as a red solid (125 mg, 75 % yield). ^{1}H NMR (500 MHz, DMSO-d_6) δ 7.80 (s, 1H), 7.78 (d, J = 7.5 Hz, 1H), 7.75 (d, J = 8.0 Hz, 2H), 7.76 – 7.70 (m, 3H), 7.49 (d, J = 4.0 Hz, 1H), 7.51 – 7.48 (m, 1H), 7.41 (d, J = 8.5 Hz, 2H), 5.29 (s, 1H), 4.54 (s, 2H), 4.03 (s, 2H); ^{13}C NMR (125 MHz, DMSO-d_6) δ 191.9, 148.6, 148.4, 142.7, 137.5, 137.3, 135.2, 134.2, 131.9, 130.8, 126.6, 126.2, 125.4, 124.8, 124.1, 122.9, 61.9, 31.3. HRMS (ESI) *calcd* for $C_{21}H_{17}O_2S$ $[M + H]^+$ 333.0944, found, 333.0943.

(*Z*)-2-((5-(3-Aminophenyl)thiophen-2-yl)methylene)-2,3-dihydro-1H-inden-1-one (**38**). Prepared by **Method 3** with intermediate **36A** (152 mg, 0.5 mmol) and 3-aminophenylboronic acid (137 mg, 1.0 mmol) to afford compound **38** as a yellow solid (100 mg, 68% yield). ^{1}H NMR (600 MHz, DMSO-d_6) δ 7.80 (t, J = 1.8 Hz, 1H), 7.78 (d, J = 7.2 Hz, 1H), 7.72 (d, J = 3.6 Hz, 2H), 7.68 (d, J = 4.2 Hz, 1H), 7.53 (d, J = 3.6 Hz, 1H), 7.50-7.48 (m, 1H), 7.11 (t, J = 7.8 Hz, 1H), 6.96 (t, J = 1.8 Hz, 1H), 6.94 (d, J = 7.2 Hz, 1H), 6.59 (dd, J_1 = 1.8 Hz, J_2 = 7.8 Hz, 1H), 5.33 (s, 2H), 4.01 (s, 2H); ^{13}C NMR (150 MHz, DMSO-d_6) δ 193.0, 150.6, 149.9, 149.6, 138.2, 136.2, 135.2, 132.7, 130.2, 127.3, 126.6, 124.7, 123.9, 114.9, 13.7, 111.1, 32.4. HRMS (ESI) *calcd* for $C_{20}H_{16}NOS$ $[M + H]^+$ 318.0947, found, 318.0937.

(*Z*)-2-((5-(4-Hydroxy-3-methoxyphenyl)thiophen-2-yl)methylene)-2,3-dihydro-1H-inden-1-one (**39**). Prepared by **Method 3** with intermediate **36A** (152 mg, 0.5 mmol) and 4-hydroxy-3-methoxyphenylboronic acid pinacol ester (250 mg, 1.0 mmol) to afford compound **39** as a red solid (124 mg, 71% yield). ^{1}H NMR (600 MHz, DMSO-d_6) δ 7.77 (d, J = 8.4 Hz, 2H), 7.75 – 7.69 (m, 2H), 7.67 (d, J = 3.6 Hz, 1H), 7.56 (d, J = 3.6 Hz,

1H), 7.49 (td, $J1$ = 1.2 Hz, $J2$ = 7.8 Hz, 1H), 7.28 (d, J = 1.8 Hz, 1H), 7.21 (dd, $J1$ = 1.8 Hz, $J2$ = 7.8 Hz, 1H), 6.85 (d, J = 7.8 Hz, 1H), 4.01 (s, 2H), 3.88 (s, 3H); ^{13}C NMR (150 MHz, DMSO-d_6) δ 193.0, 150.7, 149.6, 148.7, 138.5, 137.3, 136.4, 135.1, 132.1 128.2, 127.2, 126.7, 124.0, 123.9, 119.5, 116.6, 110.3, 56.3, 32.3. HRMS (ESI) *calcd* for $C_{21}H_{17}O_3S$ $[M + H]^+$ 349.0893, found, 349.0881.

(*Z*)-2-((5-(4-(Dimethylamino)phenyl)thiophen-2-yl)methylene)-2,3-dihydro-1H-inden-1-one (**40**). Prepared by **Method 3** with intermediate **36A** (152 mg, 0.5 mmol) and 4- (N,N-dimethylamino)phenylboronic acid pinacol ester (247 mg, 1.0 mmol) to afford compound **40** as a red solid (118 mg, 68% yield). ^{1}H NMR (600 MHz, DMSO-d_6) δ 7.77 (d, J = 7.8 Hz, 2H), 7.74 – 7.71 (m, 2H), 7.65 (d, J = 4.2 Hz, 1H), 7.61 (d, J = 9.0 Hz, 2H), 7.50 – 7.48 (m, 2H), 6.78 (d, J = 8.4 Hz, 2H), 4.01 (s, 2H), 2.99 (s, 6H); ^{13}C NMR (150 MHz, $CDCl_3$ + DMSO-d_6) δ 190.8, 149.2, 148.8, 147.6, 147.1, 136.6, 134.4, 133.8, 133.7, 129.3, 125.0, 124.9, 120.1, 119.2, 110.5, 38.3, 30.4. HRMS (ESI) *calcd* for $C_{22}H_{20}NOS$ $[M + H]^+$ 346.1260, found, 346.1259.

(*Z*)-2-((5-(2-(Dimethylamino)pyrimidin-5-yl)thiophen-2-yl)methylene)-2,3-dihydro-1H-inden-1-one (**41**). Prepared by **Method 3** with intermediate **36A** (152 mg, 0.5 mmol) and 2-(dimethylamino)pyrimidine-5-boronic acid pinacol ester (249 mg, 1.0 mmol) to afford compound **41** as a red solid (72 mg, 40%). ^{1}H NMR (600 MHz, DMSO-d_6) δ 8.76 (s, 2H), 7.78 (s, 1H), 7.72 – 7.70 (m, 3H), 7.58 (d, J = 4.2 Hz, 1H), 7.50 – 7.48 (m, 1H), 4.00 (s, 2H), 3.19 (s, 6H); ^{13}C NMR (150 MHz, $CDCl_3$) δ 193.6, 161.2, 154.8, 148.9,

144.4, 138.7, 138.1, 134.5, 134.4, 132.2, 127.6, 126.5, 126.2, 124.2, 122.6, 115.9, 37.2, 32.3. HRMS (ESI) *calcd* for $C_{20}H_{18}N_3OS$ $[M + H]^+$ 348.1165, found, 348.1165.

(*Z*)-2-((5-(2,4-Dimethoxypyrimidin-5-yl)thiophen-2-yl)methylene)-2,3-dihydro-1H-inden-1-one (**42**). Prepared by **Method 3** with intermediate **36A** (152 mg, 0.5 mmol) and 2,4-dimethoxy-5-pyrimidinylboronic acid (184 mg, 1.0 mmol) to afford compound **42** as a red solid (124 mg, 68 % yield). ^{1}H NMR (600 MHz, $CDCl_3$) δ 8.59 (s, 1H), 7.89 (d, *J* = 7.2 Hz, 1H), 7.85 (s, 1H), 7.62 (t, *J* = 7.2 Hz, 1H), 7.58 (d, *J* = 7.8 Hz, 1H), 7.48 (d, *J* = 4.2 Hz, 1H), 7.43 (t, *J* = 7.2 Hz, 1H), 7.40 (d, *J* = 4.2 Hz, 1H), 4.13(s, 3H), 4.06 (s, 3H), 3.97 (s, 2H); ^{13}C NMR (150 MHz, $CDCl_3$) δ 193.6, 166.8, 164.5, 156.3, 148.9, 139.9, 139.4, 138.6, 134.5, 133.6, 132.7, 127.7, 126.5 126.3, 126.2, 124.3, 109.9, 55.1, 54.5, 32.4. HRMS (ESI) *calcd* for $C_{20}H_{17}N_2O_3S$ $[M + H]^+$ 365.0954, found, 365.0939.

(*Z*)-2-((5-(2-(Dimethylamino)pyrimidin-5-yl)thiophen-2-yl)methylene)-6-hydroxy-2,3-dihydro-1H-inden-1-one (**43**). Prepared by **Method 3** with intermediate **36B** (160 mg, 0.5 mmol) and 2-(dimethylamino)pyrimidine-5-boronic acid pinacol ester (249 mg, 1.0 mmol) to afford compound **43** as a red solid (79 mg, 44% yield). ^{1}H NMR (600 MHz, $CDCl_3$) δ 8.75 (s, 2H), 7.68 (s, 1H), 7.64 (d, *J* = 3.6 Hz, 1H), 7.56 (d, *J* = 3.6 Hz, 1H), 7.39 (d, *J* = 7.8 Hz, 1H), 7.04 (d, *J* = 8.4 Hz, 1H), 6.96 (s, 1H), 3.82 (s, 2H), 3.19 (s, 6H); ^{13}C NMR (150 MHz, DMSO-d_6 + Methanol-d_4) δ 193.9, 161.5, 158.4, 154.9, 143.5, 139.6, 138.2, 134.9, 134.6, 127.6, 126.4, 124.5, 123.4, 116.1, 109.9, 36.7, 31.3. HRMS (ESI) *calcd* for $C_{20}H_{17}N_3O_2S$ $[M + K]^+$ 402.0673, found, 402.0673.

(*Z*)-6-Hydroxy-2-((5-(4-(hydroxymethyl)phenyl)thiophen-2-yl)methylene)-2,3-dihydro-1H-inden-1-one (**44**). Prepared by **Method 3** with intermediate **36B** (160 mg, 0.5 mmol) and 4-(hydroxymethyl)phenylboronic acid pinacol ester (234 mg, 1.0 mmol) to afford compound **44** as a brown solid (131 mg, 75 % yield). ^{1}H NMR (500 MHz, DMSO-d_6) δ 7.73 (d, J = 8.0 Hz, 2H), 7.67 (s, 1H), 7.64 (s, 2H), 7.40 (d, J = 8.5 Hz, 2H), 7.34 (d, J = 8.0 Hz, 1H), 6.99 (dd, $J1$ = 2.5 Hz, $J2$ = 8.5 Hz, 1H), 6.89 (d, J = 2.0 Hz, 1H), 4.53 (s, 2H), 3.82 (s, 2H); ^{13}C NMR (125 MHz, DMSO-d_6) δ 192.4, 147.7, 142.6, 138.6, 137.9, 134.5, 133.8, 130.9, 126.6, 126.1, 124.7, 124.0, 123.9, 108.0, 61.9, 30.5. HRMS (ESI) *calcd* for $C_{21}H_{17}O_3S$ $[M + H]^+$ 349.0893, found, 349.0793.

(*Z*)-2-((4-Bromothiophen-2-yl)methylene)-2,3-dihydro-1H-inden-1-one (**45**). Prepared by **Method 2** with 1- indanone (650 mg, 5.0 mmol) and 4-bromo-2-thiophenecarboxaldehyde (1.4 g, 7.5 mmol) to afford intermediate **45** as a yellow solid (1.5 g, 92%). ^{1}H NMR (500 MHz, $CDCl_3$) δ 7.90 (d, J = 7.5 Hz, 1H), 7.75 (s, 1H), 7.64 (td, $J1$ = 1.0 Hz, $J2$ = 7.5 Hz, 1H), 7.57 (d, J = 7.5 Hz, 1H), 7.45 (s, 1H), 7.43 (d, J = 7.0 Hz, 1H), 7.33 (s, 1H), 3.92 (s, 2H); ^{13}C NMR (125 MHz, $CDCl_3$) δ 193.5, 148.9, 140.8, 138.2, 134.9, 134.23, 134.2, 127.9, 127.1, 126.3, 124.9, 124.5, 111.6, 32.2. HRMS (ESI) *calcd* for $C_{14}H_{10}BrOS$ $[M + H]^+$ 304.9630, found, 304.9625.

(*Z*)-2-((4-(4-(Hydroxymethyl)phenyl)thiophen-2-yl)methylene)-2,3-dihydro-1H-inden-1-one (**46**). Prepared by **Method 3** with intermediate **45** (152 mg, 0.5 mmol) and 4-(hydroxymethyl)phenylboronic acid pinacol ester (234 mg, 1.0 mmol) to afford compound **46** as a brown solid (110 mg, 66% yield). ^{1}H NMR (500 MHz, DMSO-d_6) δ 8.24 (s, 1H),

8.11 (s, 1H), 7.82 (s, 1H), 7.78 (d, *J* = 7.5 Hz, 1H), 7.76 – 7.69 (m, 4H), 7.51-7.48 (m, 1H), 7.39 (d, *J* = 8.0 Hz, 2H), 5.23 (s, 1H), 4.53 (s, 2H), 4.02 (s, 2H); ^{13}C NMR (125 MHz, DMSO-d_6) δ 192.1, 148.7, 141.7, 141.5, 139.1, 137.1, 134.3, 132.5, 132.1, 127.2, 126.4, 126.2, 125.8, 125.2, 125.1, 122.9, 61.9, 31.1. HRMS (ESI) *calcd* for $C_{21}H_{17}O_2S$ $[M + H]^+$ 333.0944, found, 333.0943.

(*Z*)-2-((4-(Pyridin-3-yl)thiophen-2-yl)methylene)-2,3-dihydro-1H-inden-1-one (**47**). Prepared by **Method 3** with intermediate **45** (152 mg, 0.5 mmol) and 3-pyridineboronic acid pinacol ester (234 mg, 1.0 mmol) to afford compound **47** as a red solid (100 mg, 66% yield). ^{1}H NMR (500 MHz, DMSO-d_6) δ 8.03 (s, 1H), 8.00 (s, 1H), 7.80 (s, 1H), 7.70 (d, *J* = 7.5 Hz, 1H), 7.74 – 7.71 (m, 3H), 7.57 (d, *J* = 8.5 Hz, 2H), 7.50-7.47 (m, 1H), 6.82 (d, *J* = 8.5 Hz, 2H), 3.99 (s, 2H); ^{13}C NMR (125 MHz, DMSO-d_6) δ 193.2, 149.7, 139.9, 138.3, 135.3, 133.3, 132.7, 128.2, 127.8, 127.3, 126.4, 123.9, 116.3, 32.2. HRMS (ESI) *calcd* for $C_{19}H_{14}NOS$ $[M + H]^+$ 304.0791, found, 304.0788.

(*Z*)-2-((5-Bromothiophen-2-yl)methylene)-3,4-dihydronaphthalen-1(2H)-one (**48**). Prepared by **Method 1** with alpha-tetralone (730 mg, 5.0 mmol) and 5-bromo-2-thiophenecarboxaldehyde (1.4 g, 7.5 mmol) to afford intermediate **48** as a yellow solid (1.3 g, 82% yield). ^{1}H NMR (600 MHz, $CDCl_3$) δ 8.09 (d, *J* = 7.8 Hz, 1H), 7.90 (s, 1H), 7.49 (t, *J* = 7.2 Hz, 1H), 7.36 (t, *J* = 7.2 Hz, 1H), 7.27 (d, *J* = 7.8 Hz, 1H), 7.13 (d, *J* = 4.2 Hz, 1H), 7.09 (d, *J* = 4.2 Hz, 1H), 3.11 (t, *J* = 6.6 Hz, 2H), 3.02 (t, *J* = 6.6 Hz, 2H); ^{13}C NMR (150 MHz, $CDCl_3$) δ 186.9, 142.9, 140.7, 133.5, 133.3, 132.2, 130.5, 128.8, 128.2, 128.1, 127.1,

116.9, 28.0, 27.2. HRMS (ESI) *calcd* for $C_{15}H_{12}BrOS$ $[M + H]^+$ 318.9787, found, 318.9788.

(*Z*)-2-((5-(4-(Hydroxymethyl)phenyl)thiophen-2-yl)methylene)-3,4-dihydronaphthalen-1(2H)-one (**49**). Prepared by **Method 3** with intermediate **48** (159 mg, 0.5 mmol) and 4-hydroxy-3-methoxyphenylboronic acid pinacol ester (234 mg, 1.0 mmol) to afford compound **49** as a red solid (125 mg, 72% yield). ^{1}H NMR (600 MHz, $CDCl_3$) δ 8.13 (d, *J* = 7.2 Hz, 1H), 8.03 (s, 1H), 7.67 (d, *J* = 7.8 Hz, 2H), 7.51 (t, *J* = 7.8 Hz, 1H), 7.43 (d, *J* = 7.8 Hz, 2H), 7.38 (d, *J* = 4.2 Hz, 2H), 7.36 (d, *J* = 4.2 Hz, 1H), 7.30 (d, *J* = 7.8 Hz, 1H), 4.75 (d, *J* = 5.4 Hz, 2H), 3.27 (t, *J* = 6.6 Hz, 2H), 3.07 (t, *J* = 6.6 Hz, 2H), 1.73 (t, *J* = 5.4 Hz, 1H); ^{13}C NMR (150 MHz, $CDCl_3$) δ 187.1, 148.0, 143.0, 138.5, 134.8, 133.1, 129.6, 128.2, 128.1, 127.6, 127.1, 126.1, 123.6, 64.9, 28.2, 27.2. HRMS (ESI) *calcd* for $C_{22}H_{19}O_2S$ $[M + H]^+$ 347.1100, found, 347.1089.

(*Z*)-2-((5-(4-Hydroxy-3-methoxyphenyl)thiophen-2-yl)methylene)-3,4-dihydronaphthalen-1(2H)-one (**50**). Prepared by **Method 3** with intermediate **48** (159 mg, 0.5 mmol) and 4-hydroxy-3-methoxyphenylboronic acid pinacol ester (250 mg, 1.0 mmol) to afford compound **50** as a red solid (138 mg, 76% yield). ^{1}H NMR (600 MHz, DMSO-d_6) δ 7.93 (d, *J* = 7.2 Hz, 1H), 7.88 (s, 1H), 7.55 (td, *J*1 = 1.2 Hz, *J*2 = 7.2 Hz, 1H), 7.51 (d, *J* = 3.6 Hz, 1H), 7.39 (t, *J* = 7.8 Hz, 2H), 7.27 (d, *J* = 3.6 Hz, 1H), 7.06 (dd, J_1 = 2.4 Hz, J_2 = 8.4 Hz, 1H), 7.02 (s, 1H), 6.47 (s, 1H), 3.75 (s, 3H), 3.15 (t, *J* = 6.6 Hz, 2H), 3.03 (t, *J* = 6.6 Hz, 2H); ^{13}C NMR (150 MHz, $CDCl_3$) δ 193.0, 150.7, 149.6, 148.7, 138.5,

136.4, 135.1, 132.1, 128.2, 127.2, 126.7, 124.0, 123.9, 119.5, 116.6, 110.3, 56.3, 32.3. HRMS (ESI) *calcd* for $C_{22}H_{19}O_3S$ $[M + H]^+$ 363.1049, found, 363.1039.

(*Z*)-2-((5-(2-(Dimethylamino)pyrimidin-5-yl)thiophen-2-yl)methylene)-3,4-dihydronaphthalen-1(2H)-one (**51**). Prepared by **Method 3** with intermediate **48** (159 mg, 0.5 mmol) and 2-(dimethylamino)pyrimidine-5-boronic acid pinacol ester (249 mg, 1.0 mmol) to afford compound 51 as a red solid (130 mg, 72% yield). ^{1}H NMR (600 MHz, $CDCl_3$) δ 8.58 (s, 2H), 8.11 (d, *J* = 7.8 Hz, 1H), 8.01 (s, 1H), 7.49 (t, *J* = 7.2 Hz, 1H), 7.37-7.36 (m, 2H), 7.28 (d, *J* = 7.8 Hz, 1H), 7.18 (d, *J* = 3.0 Hz, 1H), 3.25 (s, 8H), 3.06 (t, *J* = 6.6 Hz, 2H); ^{13}C NMR (150 MHz, $CDCl_3$) δ 187.0, 161.5, 154.9, 143.1, 142.9, 137.5, 134.9, 133.8, 133.1, 131.2, 129.5, 128.1, 128.0, 127.1, 122.1, 116.1, 37.3, 28.2, 27.1. HRMS (ESI) *calcd* for $C_{21}H_{20}N_3OS$ $[M + H]^+$ 362.1322, found, 362.1310.

2-((1-Chloro-3,4-dihydronaphthalen-2-yl)methylene)-1H-indene-1,3(2H)-dione (**52**). Prepared by **Method 2** with 1,3-indandione (146 mg, 1.0 mmol) and 1-chloro-3,4-dihydro-2-naphthalenecarbaldehyde (193 mg, 1.0 mmol) to afford compound **52** as a brown solid (268 mg, 81% yield). ^{1}H NMR (600 MHz, $CDCl_3$) δ 7.95 (s, 1H), 7.69-7.67 (m, 1H), 7.63-7.62 (m, 1H), 7.48-7.46 (m, 3H), 7.03-6.98 (m, 2H), 6.91-6.89 (m, 1H), 2.84 (t, *J* = 7.2, Hz, 2H), 2.60 (t, *J* = 7.2, Hz, 2H); ^{13}C NMR (150 MHz, $CDCl_3$) δ 189.6, 188.3, 142.5, 141.9, 140.0, 138.6, 134.9, 134.8, 132.4, 131.9, 130.4, 129.4, 126.9, 126.7, 126.5, 122.9, 122.8, 28.7, 27.6. HRMS (ESI) *calcd* for $C_{20}H_{14}ClO_2$ $[M + H]^+$ 321.0677, found, 321.0676.

2-((6-Methyl-4-oxo-4H-chromen-3-yl)methylene)-1H-indene-1,3(2H)-dione (**53**). Prepared by **Method 2** with 1,3- indandione (146 mg, 1.0 mmol) and 3-formyl-6-methylchromone (188 mg, 1.0 mmol) to afford compound **53** as a yellow solid (253 mg, 80% yield). ^{1}H NMR (500 MHz, $CDCl_3$) δ 10.35 (s, 1H), 8.39 (s, 1H), 8.05 (d, J = 1.0 Hz, 1H), 7.99 – 7.97 (m, 2H), 7.83 – 7.79 (m, 2H), 7.52 (dd, J_1 = 1.5 Hz, J_2 = 7.0 Hz, 1H), 7.43 (d, J = 7.0 Hz, 1H), 2.46 (s, 3H); ^{13}C NMR (125 MHz, $CDCl_3$) δ 190.1, 189.1, 175.3, 163.4, 154.3, 142.1, 140.3, 136.7, 136.6, 135.6, 135.5, 135.3, 129.0, 125.9, 123.6, 123.5, 123.3, 118.4, 118.3, 21.0. HRMS (ESI) *calcd* for $C_{20}H_{13}O_4$ $[M + H]^+$ 317.0808, found, 317.0808.

2-((6-Bromo-4-oxo-4H-chromen-3-yl)methylene)-1H-indene-1,3(2H)-dione (**54**). Prepared by **Method 2** with 1,3- indandione (100 mg, 0.7 mmol) and 6-bromo-3-formylchromone (173 mg, 0.7 mmol) to afford compound **54** as a yellow solid (230 mg, 72% yield). ^{1}H NMR (500 MHz, $CDCl_3$) δ 10.35 (s, 1H), 8.39 (s, 1H), 8.05 (d, J = 1.0 Hz, 1H), 7.99 – 7.97 (m, 2H), 7.83 – 7.79 (m, 2H), 7.52 (dd, J_1 = 1.5 Hz, J_2 = 7.0 Hz, 1H), 7.43 (d, J = 7.0 Hz, 1H), 2.46 (s, 3H); ^{13}C NMR (150 MHz, $CDCl_3$ + DMSO-d_6) δ 194.4, 193.6, 178.7, 159.7, 146.9, 144.9, 142.7, 142.6, 141.0, 140.9, 139.4, 139.2, 134.7, 133.3, 133.2, 129.9, 128.5, 126.4, 124.4, 123.8, 122.9, 116.1. HRMS (ESI) *calcd* for $C_{19}H_{10}BrO_4$ $[M + H]^+$ 380.9757, found, 380.9756.

2-((1H-Indol-2-yl)methylene)-1H-indene-1,3(2H)-dione (**55**). Prepared by Method 2 with 1,3-indandione (146 mg, mmol) and indole-2-carboxaldehyde (145 mg, 1.0 mmol) to afford compound **55** as a yellow solid (255 mg, 81% yield). ^{1}H NMR (500 MHz,

DMSO-d_6) δ 12.2 (s, 1H), 8.03–8.01 (m, 1H), 7.96 – 7.95 (m, 3H), 7.91 (d, *J* = 5.5 Hz, 1H), 7.75 – 7.71 (m, 3H), 7.41 – 7.38 (m, 1H), 7.16 – 7.12 (m, 1H); ^{13}C NMR (125 MHz, DMSO-d_6) δ 191.2, 189.8, 141.6, 140.4, 139.9, 136.4, 133.8, 133.4, 128.5, 128.1, 124.9, 123.5, 123.3, 122.9, 121.6, 119.5, 113.6. HRMS (ESI) *calcd* for $C_{18}H_{12}NO_2$ $[M + H]^+$ 274.0863, found, 274.0862.

2-((3-(4-Bromophenyl)isoxazol-5-yl)methylene)-1H-indene-1,3(2H)-dione (**56**). Prepared by **Method 2** with 1,3- indandione (146 mg, 1.0 mmol) and 3-(4-bromophenyl)isoxazole-5-carboxaldehyde (252 mg, 1.0 mmol) to afford compound **56** as a yellow solid (238 mg, 63% yield). ^{1}H NMR (500 MHz, $CDCl_3$) δ 8.36 (s, 1H), 8.07. – 8.05 (m, 2H), 8.02 – 8.01 (m, 2H), 7.92 (d, *J* = 8.5 Hz, 2H), 7.79 (d, *J* = 8.0 Hz, 2H), 7.65 (s, 1H); ^{13}C NMR (125 MHz, $CDCl_3$) δ 188.4, 187.9, 165.7, 162.8, 142.8, 140.8, 137.1, 136.9, 132.9, 132.8, 129.2, 127.4, 124.7, 124.0, 123.9, 122.9, 110.1. HRMS (ESI) *calcd* for $C_{19}H_{11}BrNO_3$ $[M + H]^+$ 379.9917, found, 379.9910.

(*Z*)-3-((6-Hydroxy-1-oxo-1,3-dihydro-2H-inden-2-ylidene)methyl)-6-methyl-4H-chromen-4-one (**57**). Prepared by Method 1 with 6-hydro-indanone (148 mg, 1.0 mmol) and 3-formyl-6-methylchromone (188 mg, 1.0 mmol) to afford compound 57 as a yellow solid (290 mg, 82% yield). ^{1}H NMR (600 MHz, DMSO-d_6) δ 9.87 (s, 1H), 8.82 (s, 1H), 7.90 (d, *J* = 0.6 Hz, 1H), 7.65 (dd, J_1 = 1.8 Hz, J_2 = 8.4 Hz, 1H), 7.61 (d, *J* = 8.4 Hz, 1H), 7.58 (t, *J* = 1.8 Hz, 1H), 7.44 (d, *J* = 7.8 Hz, 1H), 7.14 (dd, J_1 = 2.4 Hz, J_2 = 7.8 Hz, 1H), 7.07 (d, *J* = 2.4 Hz, 1H), 3.90 (d, *J* = 1.8 Hz, 2H), 2.43 (s, 3H); ^{13}C NMR (150 MHz, DMSO-d_6) δ 193.2, 175.5, 158.0, 157.6, 154.2, 140.9, 138.9, 136.9, 136.2, 127.8, 125.2,

124.1, 123.2, 122.8, 119.6, 118.8, 108.7, 31.4, 20.9. HRMS (ESI) *calcd* for $C_{20}H_{15}O_4$ $[M + H]^+$ 319.0965, found, 319.0964.

(*Z*)-3-((6-Methyl-4-oxo-4H-chromen-2-yl)methylene)indolin-2-one (**58**). Prepared by **Method 1** with 2-oxindole (200 mg, 1.5 mmol) and 3-formyl-6-methylchromone (283 mg, 1.5 mmol) to afford compound **58** as a yellow solid (310 mg, 68% yield). ^{1}H NMR (600 MHz, DMSO-d_6) δ 10.74 (s, 1H), 9.95 (d, J = 0.6 Hz, 1H), 7.95 (s, 1H), 7.78 (s, 1H), 7.71 – 7.64 (m, 3H), 7.25 (td, $J1$ = 1.2 Hz, $J2$ = 7.8 Hz, 1H), 7.02 (t, J = 7.8 Hz, 1H), 6.85 (d, J = 8.4 Hz, 1H), 2.46 (s, 3H); ^{13}C NMR (150 MHz, DMSO-d_6) δ 175.4, 168.0, 160.4, 154.3, 141.2, 136.3, 136.1, 129.9, 127.9, 125.8, 125.2, 124.6, 123.3, 121.9, 120.4, 119.0, 117.6, 110.1, 20.9. HRMS (ESI) *calcd* for $C_{19}H_{14}NO_3$ $[M + H]^+$ 304.0968, found, 304.0968.

4.2. α-Synuclein fibril formation

Fibrils were made from α-synuclein peptide (R-peptide, Bogart, GA) as follows: α-Synuclein peptide (0.5 mg) was suspended in 0.2 ml water and transferred into a centricon (10000 MWCO). 0.2 mL phosphate buffer (10 mM, pH 7.5) was added to this suspension was added, and any soluble materials were removed by spinning for 5 minutes in a centrifuge (18000g). The process was repeated four times. After the fourth time, the peptide was transferred into a microtube (200 µl), and 2.5 µl of 300 mM $MnCl_2$ (made in water) was added. The resulting mixture was stirred at 40 ^{0}C in an incubator for seven days until the solution turned hazy. The fibrils were spun down at 21000 rcf for six

minutes. The supernatant was decanted and tested for monomer concentration using the BCA assay, and the fibril pellet was resuspended in 200 µl PBS buffer (pH = 7.4). Analysis BCA assay data showed a final concentration of peptide 129.6 µM in fibrils.

4.3. α-Synuclein fibril/ligand binding assay

The fluorescence (F_1) of ligand solutions at various concentrations (0.1 nM to 10 µM) in PBS (pH = 7.5, 196.2 µL) were recorded and then transferred into microtube containing α-synuclein fibrils (3.8 µL, 2.5 µM final concentration). The mixture was incubated at 37 ^{0}C for 1 hour with shaking. Then the mixture was spun down at 21000g for 15 minutes to separate the fibrils. The supernatant was decanted, and its fluorescence (F_2) was measured. The fluorescence (F_3) of the bound fraction was obtained by subtracting F_2 from F_1. All data points were performed in triplicate. The dissociation constant (K_d) was determined by fitting the data to the equation $Y = B_{max} \times X/(X + K_d)$, [where Y = fluorescence units of the bound fraction (F3) and X = ligand concentration], by nonlinear regression using MATLAB software (R2019B).

4.4. Aβ fibrils formation

Aβ (1–40) peptide (R-Peptide, Bogart, GA), was dissolved in PBS, pH 7.4, to a final concentration of 433 µg/ml (100 µM). The solution was stirred using a magnetic stir bar at 700 rpm for four days at room temperature to drive fibrils' formation. The fibrils were spun down at 21000 rcf for six minutes. The supernatant was decanted and tested for monomer concentration using the BCA assay. BCA assay data showed a final concentration of

peptide 129.6 µM in fibrils. The stock solution was aliquoted and stored at -80 ^{o}C for future use. The stock solutions were stirred thoroughly before removing aliquots for binding assays, to maintain a homogenous suspension of fibrils.

4.5. Aβ fibril/ligand binding assay

Ligand solutions at various concentrations from 1 nM to 100 µM in PBS (pH = 7.5, 180 µL) ware added into microtube containing Aβ fibrils (20 µL, 10 µM final concentration). The mixture was incubated at 37 ^{0}C for 1 hour with shaking and then spun down at 21000g for 12 minutes to separate the fibrils. The precipitate was washed twice with Tris-HCl and resuspended in 200 µL buffer. Fluorescence was measured in a SpectraMax-384 plate reader using excitation and emission maxima of the molecule. All data points were performed in triplicate. The dissociation constant (K_d) was determined by fitting the data to the equation $Y = B_{max} \times X/(X + K_d)$, by nonlinear regression using MATLAB software (R2019B).

4.6. Labeling of α-synuclein aggregates in Human PD Brain Tissue

Confirmed PD and AD (as well as control) tissue specimens were obtained from the NIH Brain & Tissue Repository-California, Human Brain & Spinal Fluid Resource Center, VA West Los Angeles Medical Center, Los Angeles, California, which is supported in part by National Institutes of Health and the US Department of Veterans Affairs.

Fresh frozen tissue from the frontal cortex was embedded in Tissue-Tek O.C.T. and kept in the liquid nitrogen for 30 minutes. The embedded tissue was sliced into 30 µm thick

sections with Lecia Biosystems Cryostats under -20 ºC and mounted onto microscope slides, washed with 1× PBST, and then fixed with 10% formalin solution for 20 minutes. Following fixation, the section was washed with 1× PBS (three times) and permeablized with 0.1% Triton-X 100 for ten minutes, followed by a washed with 1× PBS. Tissue was then incubated with 2% normal Donkey serum at room temperature for one hour followed by incubation with antibody Syn211(Ascites free) (1:1000 in 1% Donkey serum) overnight at 4 °C. Tissue was washed with 1× PBS and incubated for two hours at room temperature with Alexa Fluor 647 labeled secondary antibody (1:200 in PBS). After a washed with 1× PBST, tissue was incubated at room temperature for thirty minutes with 5 μM of test compound dissolved in PBS. The section was washed with 1× PBST, treated with TrueBlack Linpofuscin Autofluorescence Quencher (1:20 in ethanol) for two minutes, washed with 1× PBS, coverslipped, and imaged in Olympus IX81 microscope using standard excitation/emission filters.

4.7. Staining of amyloid-β plaques in human AD brain tissue

Fresh frozen tissue from the frontal cortex was embedded with Tissue-Tek O.C.T. Compound and kept in the liquid nitrogen for 30 minutes. The embedded tissue was sliced into 30 μm thick sections with Lecia Biosystems Cryostats under -20 ºC and mounted onto microscope slides. The section was washed with 1× PBST and then fixed with 10% formalin solution for twenty minutes. It was then permeablized with 0.1% Triton-X 100 for ten minutes, incubated with 2% normal donkey serum at room temperature for one hour, followed by incubation with purified anti-β-Amyloid, 17-24 Antibody (Covance,

4G8) (1:500 in 1% Donkey serum) overnight at 4 °C. The section was incubated for two hours at room temperature with Alexa Fluor 647 labeled secondary (1:200 in PBS) and then treated with the compound to be tested. Each tissue section was incubated at room temperature for thirty minutes with 5 μM of test compound dissolved in PBS and then treated with TrueBlack Linpofuscin Autofluorescence Quencher (Biotium, 1:20 in ethanol) for two minutes. Finally, tissue was washed, coverslipped, and imaged in an Olympus IX81 microscope using standard excitation/emission filters.

4.8. Determination of Pearson's Correlation Coefficients (PCC) in tissue mages.

PCC values in the composite images were determined using the ImarisColoc module of IMARIS x64 version 9. The analysis was carried out over the entire frame of the image. A threshold for each fluorophore channel, ligand (594), and antibody (647) was defined by increasing the minimums in the LUT distribution, in a way to define the true signal. A region of interest was selected by masking the background, and all the region except the signal was masked off. All voxels excluding the region of interest defined by the masked channel were ignored for colocalization analysis. A colocalization channel was created based on the overlapping voxels using the software. Statistics for the colocalized channel generated by the software resulted in the respective Pearson's correlation coefficients.

ASSOCIATED CONTENT

Supporting Information. Supporting Information is available

^{1}H and ^{13}C NMR spectra of all compounds

2D NMR data for NOE determination of double bond geometry

Saturation α-syn and Aβ fibril binding curves to determine K_d values

Determination of fluorimetric properties of the lead ligands

Samples of microscopy images from control brain tissue with no pathology

HPLC profiles of lead compounds

AUTHOR INFORMATION

*Corresponding Author, E-mail: eatanifu@texaschildrens.org . ORCID: 0000-0001-8803-5643

Financial Conflict of Interests: XS and PA declare no competing financial interest. ZS is a stockholder at Alzeca Biosciences, Inc; JE is a stockholder at Alzeca Biosciences, Inc; AA is a stockholder and consultant at Alzeca Biosciences, Inc; ET is a stockholder and consultant at Alzeca Biosciences, Inc.

ACKNOWLEDGMENTS

A grant funded this work from Alzeca Biosciences, Inc. to AA.

Confirmed PD and AD (as well as control) tissue specimens were obtained from the NIH Brain & Tissue Repository-California, Human Brain & Spinal Fluid Resource Center, VA West Los Angeles Medical Center, Los Angeles, California, which is supported in part by National Institutes of Health and the US Department of Veterans Affairs.

The authors also acknowledge the NIH Neurobiobank for facilitating tissue acquisition.

REFERENCES

1. Ross, C. A.; Poirier, M. A. Protein Aggregation and Neurodegenerative Disease. *Nat Med* **2004**, *10 Suppl*, S10–7.

2. Irvine, G. B.; El, O. M. Protein Aggregation in the Brain: the Molecular Basis for Alzheimer's and Parkinson's Diseases. *Mol Med* **2008**, 14(7-8), 451.

3. Gelb, D. J.; Oliver, E.; Gilman, S. Diagnostic Criteria for Parkinson Disease. *Archives on Neurology* **1999**, 56 (1), 33.

4. Braak, H.; Del Tredici, K. Neuropathological Staging of Brain Pathology in Sporadic Parkinson's Disease: Separating the Wheat from the Chaff. *Journal of Parkinson's Disease* **2017**, *7*, S71.

5. Braak, H.; Ghebremedhin, E.; Rüb, U.; Bratzke, H.; Del Tredici, K. Stages in the Development of Parkinson's Disease-Related Pathology. *Cell and Tissue Research* **2004**, *318*, 121.

6. Braak, H.; Bohl, J. R.; Müller, C. M.; Rüb, U.; Del Tredici, K. Stanley Fahn Lecture 2005: the Staging Procedure for the Inclusion Body Pathology Associated with Sporadic Parkinson's Disease Reconsidered. *Movement Disorders* **2006**, *21*, 2042.

7. Ingelsson, M. Alpha-Synuclein Oligomers—Neurotoxic Molecules in Parkinson's Disease and Other Lewy Body Disorders. *Frontiers in Neuroscience* **2016**, *10*, 16.

8. Kim, W. S.; Kågedal, K.; Halliday, G. M. Alpha-Synuclein Biology in Lewy Body Diseases. *Nature Biotechnology* **2014**, *6*, 1186.

9. Beach, T. G.; Consortium, T. A. P. D.; Adler, C. H.; Lue, L.; Sue, L. I.; Bachalakuri, J.; Henry-Watson, J.; Sasse, J.; Boyer, S.; Shirohi, S.; Brooks, R.; Eschbacher, J.; White, C. L.; Akiyama, H.; Caviness, J.; Shill, H. A.; Connor, D. J.; Sabbagh, M. N.; Walker, D. G. Unified Staging System for Lewy Body Disorders: Correlation with Nigrostriatal Degeneration, Cognitive Impairment and Motor Dysfunction. *Molecular Neurobiology* **2009**, *117*, 613.

10. Kotzbauer, P. T.; Cairns, N. J.; Campbell, M. C.; Willis, A. W.; Racette, B. A.; Tabbal, S. D.; Perlmutter, J. S. Pathologic Accumulation of α-Synuclein and Aβ in Parkinson Disease Patients with Dementia. *Archives of Neurology* **2012**, *69*, 1326.

11. Morris, E.; Chalkidou, A.; Hammers, A.; Peacock, J.; Summers, J.; Keevil, S. Diagnostic Accuracy of 18F Amyloid PET Tracers for the Diagnosis of Alzheimer's Disease: a Systematic Review and Meta-Analysis. *European Journal of Nuclear Medicine and Molecular Imaging* **2015**, *43*, 374.

12. Bischof, G. N.; Endepols, H.; van Eimeren, T.; Drzezga, A. Tau-Imaging in Neurodegeneration. *Methods* **2017**, *130*, 114.

13. Mathis, C. A.; Lopresti, B. J.; Ikonomovic, M. D.; Klunk, W. E. Small-Molecule PET Tracers for Imaging Proteinopathies. *Seminars in Nuclear Medicine* **2017**, *47*, 553.

14. Kotzbauer, P. T.; Tu, Z.; Mach, R. H. Current Status of the Development of PET Radiotracers for Imaging Alpha Synuclein Aggregates in Lewy Bodies and Lewy Neurites. *Clinical and Translational Imaging* **2016**, *5*, 3.

15. Shah, M.; Seibyl, J.; Cartier, A.; Bhatt, R.; Catafau, A. M. Molecular Imaging Insights into Neurodegeneration: Focus on -Synuclein Radiotracers. *Journal of Nuclear Medicine* **2014**, *55*, 1397.

16. Pike, V. W. Considerations in the Development of Reversibly Binding PET Radioligands for Brain Imaging. *Current Medicinal Chemistry* **2016**, *23*, 1818–1869.

17. Laruelle, M. Relationships between Radiotracer Properties and Image Quality in Molecular Imaging of the Brain with Positron Emission Tomography. *Advanced Drug Delivery Reviews* **2003**, *5*, 363.

18. Ono, M.; Doi, Y.; Watanabe, H.; Ihara, M.; Ozaki, A.; Saji, H. Structure–Activity Relationships of Radioiodinated Diphenyl Derivatives with Different Conjugated Double Bonds as Ligands for A-Synuclein Aggregates. *RSC Advances* **2016**, *6*, 44305.

19. Chu, W.; Zhou, D.; Gaba, V.; Liu, J.; Li, S.; Peng, X.; Xu, J.; Dhavale, D.; Bagchi, D. P.; d'Avignon, A.; Shakerdge, N. B.; Bacskai, B. J.; Tu, Z.; Kotzbauer, P. T.; Mach, R. H.

Design, Synthesis, and Characterization of 3-(Benzylidene)indolin-2-one Derivatives as Ligands for α-Synuclein Fibrils. *J Med Chem* **2015**, *58*, 6002.

20. Fodero-Tavoletti, M. T.; Mulligan, R. S.; Okamura, N.; Furumoto, S.; Rowe, C. C.; Kudo, Y.; Masters, C. L.; Cappai, R.; Yanai, K.; Villemagne, V. L. In Vitro Characterisation of BF227 Binding to α-synuclein/Lewy Bodies. *Molecular Neurobiology* **2009**, *617*, 54.

21. Koga, S.; Ono, M.; Sahara, N.; Higuchi, M.; Dickson, D. W. Fluorescence and Autoradiographic Evaluation of Tau PET Ligand PBB3 to A-Synuclein Pathology. *Nuklearmedizin* **2017**, *32*, 884.

22. Lengyel-Zhand, Z.; Ferrie, J. J.; Janssen, B.; Hsieh, C.-J.; Graham, T.; Xu, K.; Haney, C. M.; Lee, V. M.-Y.; John Q. Trojanowski, J. Q.; Petersson, E.J. and Mach, R. H. Synthesis and Characterization of High Affinity Fluorogenic α- Synuclein Probes. *Chemical Communications* **2020**, 56 (24), 3567-3570.

23. Xue, C.; Lin, T.Y.; Chang, D.; Guo, Z. Thioflavin T as an amyloid dye: fibril quantification, optimal concentration and effect on aggregation. *R. Soc. open sci.* **2017, 4**: 160696. http://dx.doi.org/10.1098/rsos.160696

24. Biancalana, M.; Makabe, K.; Koide, A. and Koide, S. Molecular Mechanism of Thioflavin-T Binding to the Surface of β-Rich Peptide Self-Assemblies. *J Mol Biol* **2009**; 385(4): 1052–1063. doi:10.1016/j.jmb.2008.11.006.

25. Giasson, B. I.; Jakes, R.; Goedert, M.; Duda, J. E.; Leight, S.; Trojanowski, J. Q.; and Lee, V. M. Y. A Panel of Epitope-Specific Antibodies Detects Protein Domains Distributed Throughout Human a-Synuclein in Lewy Bodies of Parkinson's Disease. *Journal of Neuroscience Research* **2000**, 59, 528–533.

26. Covell, D. J.; Robinson, J. L.; Akhtar, R. S.; Grossman, M.; Weintraub, D.; Bucklin, H. M.; Pitkin, R. M.; Riddle, D.; Yousef, A.; Trojanowski, J. Q. and Lee, V. M.-Y. Novel conformation-selective alpha-synuclein antibodies raised against different in vitro fibril forms show distinct patterns of Lewy pathology in Parkinson's disease. *Neuropathology and Applied Neurobiology* **2017**, 43, 604–620.